

Poplar Wood Formation

Genotypical influences on structure and chemistry

David Sandquist
*Faculty of Forestry,
Department of Forest Products,
Uppsala*

Doctoral Thesis
Swedish University of Agricultural Sciences
Uppsala 2011

Acta Universitatis agriculturae Sueciae
2011:1

Cover: CCRC-M1 immunolabeling of aspen wood, highlighting mainly the rays, vessels and middle lamella cell corners. The cover image shows part of a high resolution montage composed of 16 images taken from the cambium inwards.

ISSN, 1652-6880
ISBN, 978-91-576-7570-5
© 2011 David Sandquist, Uppsala
Print: Tierp 2011

Poplar Wood Formation

Abstract

Genotypical effects on wood formation in aspen (*Populus tremula x tremuloides*) have been studied at morphological, ultrastructural and micro-distributional levels. To characterize transgenically induced modifications, light-, fluorescence-, UV-, scanning- and transmission electron microscopy have been applied complemented by immunolabeling, histochemistry, multivariate statistics and image analysis. Tension wood formation in aspen has also been studied with a focus on xyloglucan micro-distribution.

To perform quantitative screening of wood immunofluorescence, a novel image analysis protocol was developed and applied. The protocol performs immunosignal isolation to calculate labeling ratio, termed coverage. Coverage is proportional to epitope availability, in relation to immunoprobe performance. The protocol was shown to perform favorably compared to operator supervised analysis and quantification.

Morphological characterization of the twelve genotypes showed significant modifications only for fiber properties. Coverage characterization showed significant modifications for LM-10 (xylan) and JIM-5 (pectin) antibody labeling. In the cell wall architecture, structure is often as important as composition. The multivariate analysis confirms previously reported relationships between individual fiber measurements, and highlights novel immunolabeling relationships. The results show that detailed morphological and coverage characterization can be a valuable addition to the semi-high throughput screening of wood tissue.

Utilizing two complementary probes the presence of xyloglucan during g-layer formation of tension wood in aspen was shown at the ultrastructural level. The observation of increased xyloglucan labeling between the g-layer and S2 strengthens the hypothesis that xyloglucan acts as conductor of tensional forces between the g-layer and the rest of the fiber wall.

Keywords: Wood formation, morphology, immunolabeling, quantification, aspen genotypes, FluoroJ, UV-microscopy, TEM, SEM, quantitative wood anatomy

Author's address: David Sandquist, SLU, Department of Forest Products,
Box 7013, 750 07 Uppsala, Sweden.
E-mail: david.sandquist@sprod.slu.se

Dedication

*To Sanna and the life that stirs within her
For sharing the journey*

Contents

Abbreviations and definitions	6
List of Publications	7
1 Introduction	9
1.1 The tree trunk	9
1.2 The annual ring	14
1.3 Hardwood tissue	14
1.4 Hardwood ultrastructure	17
1.5 Chemical composition	21
1.6 Poplar genotypes as model system	28
2 Main objectives	30
3 Materials and methods	31
3.1 Genetic transformations	31
3.2 Plant material	31
3.3 Immunolabeling for fluorescence and electron microscopy	31
3.4 Electron microscopy	34
3.5 Fluorescence microscopy	34
3.6 Light microscopy	34
3.7 Image analysis	35
3.8 Statistical analysis	36
4 Results and discussion	39
4.1 Quantification of fluorescence images	40
4.2 Morphological relationships	42
4.3 Compositional relationships	43
4.4 Genotypical influence on morphology	44
4.5 Genotypical influence on composition	45
4.6 Summary of multivariate evaluation	46
4.7 Xyloglucan deposition during aspen wood formation	47
5 Conclusions	50
6 Future work	51
References	57
Acknowledgements	58

Abbreviations and definitions

CBM	Carbohydrate binding module
MFA	Microfibril angle
ML	Middle lamella
MLcc	Middle lamella cell corner
MS	Murashige and Skoog medium
PW	Primary cell wall
S1	Outer secondary cell wall layer between PW and S2
S2	Dominating secondary cell wall layer
g-layer	Innermost (when present) reaction wood layer in hardwoods
SEM	Scanning electron microscopy
TEM	Transmission electron microscopy
FITC	Fluorescein isothiocyanate
Ultrastructure	Structural order in the range between individual molecular aggregates and entire cell walls. A common connotation is “that which is only visible at higher than light microscopy resolutions”.
UPSC	Umeå Plant Science Center

List of publications

This thesis is based on the work contained in the following papers, referred to by Roman numerals in the text:

- I David Sandquist, Jonas Hafrén, Geoffrey Daniel (2010). FluoroJ: a ImageJ plugin and protocol for quantification of immunolabeling of wood tissue. *Micron* (submitted).
- II David Sandquist, Björn Sundberg, Lennart Norell, Geoffrey Daniel (2010). Quantitative morphology and composition of twelve transgenic aspen lines down regulated for putative cell wall biosynthesis - part I morphology. (manuscript).
- III David Sandquist, Björn Sundberg, Lennart Norell, Geoffrey Daniel (2010). Quantitative morphology and composition of twelve transgenic aspen lines down regulated for putative cell wall biosynthesis - part II composition. (manuscript).
- IV David Sandquist, Lada Filonova, Laura von Schantz, Mats Ohlin, Geoffrey Daniel (2010). Microdistribution of xyloglucan in differentiating Poplar cells. *BioResources* 5(2), 796-807.

The contribution of David Sandquist to the papers included in this thesis was as follows:

- I DS compiled and wrote the FluoroJ plugin and the protocol. DS also perform and supervised the testing of the protocol.
- II DS performed all processing of material, labeling and morphological characterisation. DS together with LN developed and applied the univariate and multivariate statistical analysis.
- III DS performed all processing of material, immunolabeling, image analysis and characterisation. DS together with LN developed and applied the univariate and multivariate statistical analysis.
- IV DS grew, sampled and processed the trees. DS under the supervision of LF and GD performed all microscopy, immunolabeling and characterization.

1 Introduction

Wood is one of mans oldest and most treasured materials. As a response to environmental changes, population growth and increased living standards, there has been an accelerating trend of world demand for plant lignocelluloses (Juslin and Hansen [2003]). Particularly in recent years, the conventional use of wood for pulp, paper and construction has been further extended as a resource for bioenergy and biofuels (Vanholme et al. [2008]).

This competition for lignocellulose sees no plateauing out but rather is likely to accelerate as resources begin to dwindle and pressure from accompanying environmental concerns increases. The ability to “domesticate” trees through genetic engineering has great potential as a means for producing new clones for producing greater or modified biomass in a shorter time via enhanced growth (Hu et al. [1999], Pilate et al. [2002]).

1.1 The tree trunk

Wood can have different values and functions depending on the perspective. From a biological perspective, a tree is a evolutionary response to the race to first reach the sun. As a “function”, the “tree” has been expressed in almost every major known land plant phylum. The components that come together to make up a tree are a nutrient and water providing root system, a supportive and conducting trunk and a carbon fixing crown. The main point which separates a tree from a bush or woody plant is the size of it’s single trunk holding secondary branches clear of the ground. Along with this enhancement in size, many of the functions of trees have been further refined through evolutionary selection.

From a mechanical and chemical perspective the tree trunk, and more importantly it’s strength-providing fibers, represent a lignocellulose biopolymeric composite. Indeed, in micro-mechanical modeling the tree trunk and fibers are best described as a hydrophilic honeycombed fiber-reinforced sandwich construction (Gibson and Ashby [1999]). In summary, wood exhibits an exquisitely tailored structure and order at many discrete levels, all built from a set of simple building blocks. A visual illustration of these levels is shown in Figure 1.

In Figure 1 the different levels can be followed from the tree trunk down to individual molecules. In the trunk, many trees display two distinct areas known as heartwood and sapwood (Figure 2). Heartwood and sapwood are collectively known as xylem. Sapwood is the main water conducting tissue in a tree stem, drawing water from the root through the tracheids (in the case of softwoods) or vessels (in the case of hardwoods). Most of the cells in

Hardwood Structure

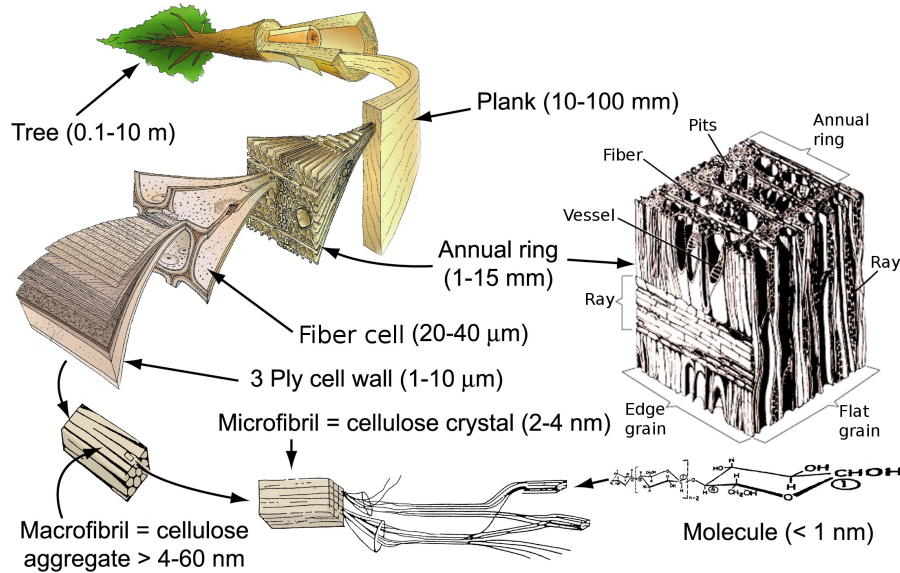


Figure 1: The many discrete layers in wood. From the left side we can follow the different layers of the tree trunk down through the xylem to the individual cellulose chains. Each of these levels have their own individual and distinct impact on the the macro-properties of wood. (Illustration adopted from J. Harrington and G. Daniel).

the xylem, such as fibers, tracheids and vessels are functional but dead. The process of development and death into functional mature cells is termed “differentiation”.

Apart from conducting water, the sapwood also contains the main storage structures. Storage in the sapwood is mainly in the rays (Figure 3), consisting of parenchyma cells which may remain alive for many years in the xylem (i.e. long after the surrounding xylem elements are dead). Rays come in many different sizes and constructions and to a large extent contribute to the different visual appearances of wood surfaces and products. In aspen the rays are particularly small, only one cell wide uniseriate and five cells high, and barely visible to the a unaided eye (Hoadley [2000]).

The other major constituent of xylem when present is heartwood, which forms from sapwood as the tree matures. In mature trees heartwood, when present, is the main strength provider of the stem (Bamber [1976], Taylor et al. [2002]). Heartwood is found in both hardwoods and softwoods (as

shown in Figure 2), but not all species exhibit heartwood formation. The time of heartwood formation differs between wood species, but the initiation of heartwood formation is not uncommon in 15-year-old sapwood. Ultimately heartwood formation is a means of energy conservation and resource management for the tree (Bamber [1976], Taylor et al. [2002]). Heartwood formation is primarily characterized by chemical changes to the storage material in the rays, a loss of water conduction in the tissue (followed by drying), and in some hardwoods by tylose formation in the vessels (Bamber [1976], Taylor et al. [2002]). All of these changes help to render the heartwood less susceptible to biodegradation as it dries and takes on a less active role in the stem.

Surrounding the outer perimeter of the stem is the bark layer (Figure 2), which is composed of phloem (inner bark) and periderm (outer bark). The periderm acts as a protective barrier between the stem and the outside environment. It provides protection against both biological attack and dehydration. The periderm is mainly composed of parenchyma and sclerenchyma (cork) cells with different composition to the xylem. Most of the cells in the periderm are functional but dead. The character and thickness of the periderm differs greatly between wood species.

Between the periderm and xylem lies the main zone in the stem of living cells, consisting of phloem and a thin layer called the vascular cambium (Figures 2 and 4). It is in the cambium that the main growth in the stem occurs. Cell division and development takes place horizontally in both the xylem and phloem directions. The cambium and the phloem are also the main conductors of the sugary sap from the leaves, converting the sugar along the way into new cells as well as providing for storage materials (i.e. for bud burst in spring).

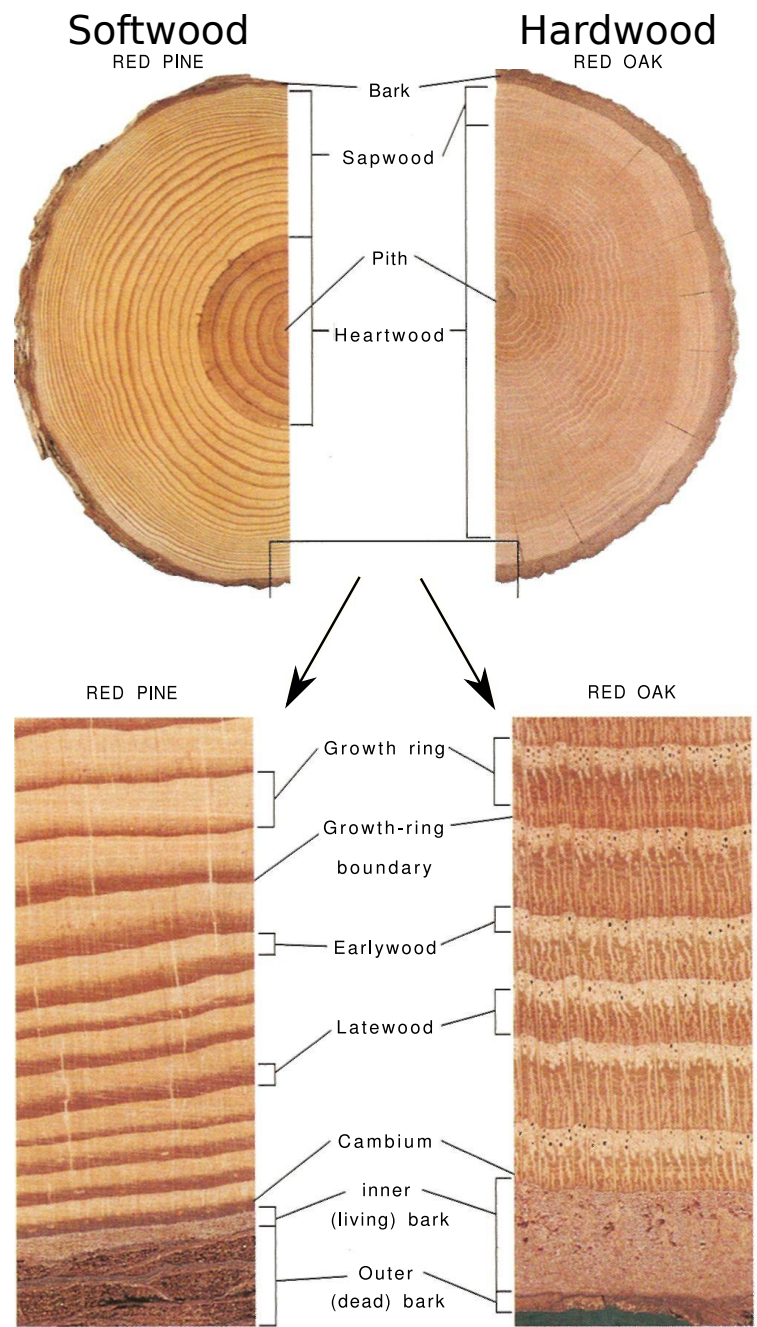


Figure 2: Illustration of tree stem and annual/growth rings. Closest to the pith is heartwood. Surrounding the heartwood is a layer of sapwood which is further connected to the cambium and bark. (Adopted from Hoadley [2000]).

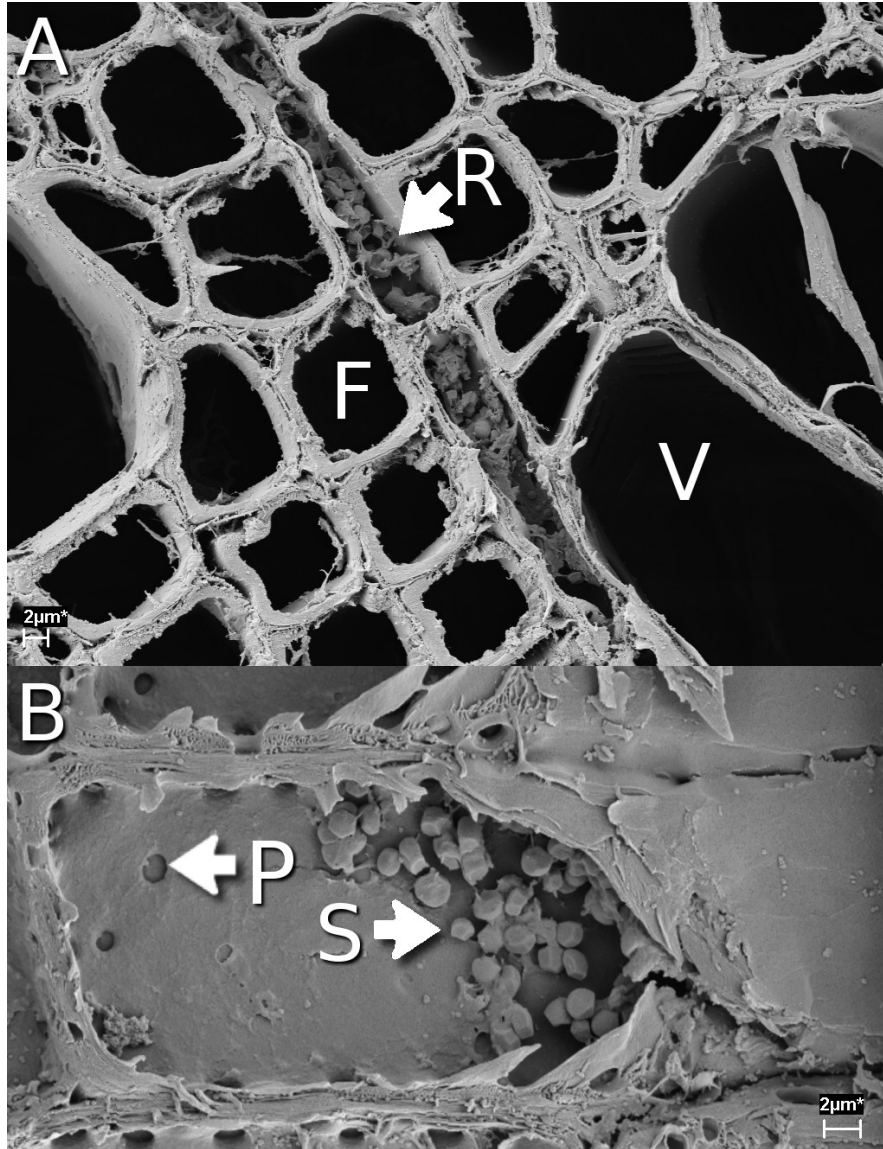


Figure 3: SEM micrographs showing ray parenchyma cell from aspen with characteristic starch granules. Transverse overview (A), with rows of ray cells (R), fibers (F) and vessels (V). Radially cut ray cell (B), showing simple pits (P) and starch storage granules (S).

1.2 The annual ring

The next level which contributes significantly to the properties of wood is the annual or growth rings (Figure 2). Many wood species in climates with distinct seasons will develop xylem with distinct zones. The properties of these zones often reflect the properties of the climate changes. In the temperate northern hemisphere, most trees show annual rings for early (spring) and late (summer) zones. For softwoods, the earlywood is dominated by large thin-walled tracheids for rapid expansion and high water conductivity. The latewood on the other hand, is dominated by thick-walled tracheids that contribute strength. The situation is similar but more complex for hardwoods and it is difficult to generalize. Some hardwood species behave similarly to softwoods with a large proportion of water conducting vessels in earlywood and more fibers in latewood (e.g. oak and beech, Figure 2). Other hardwood species show almost no difference between early- and latewood (e.g. aspen and birch).

1.3 Hardwood tissue

Below the level of annual rings is the level of individual cells and cell walls. Softwoods are made up of primarily 90-95% tracheids. In contrast hardwoods are much more complex, and exhibit more specialized cells including vessels, fibers and parenchyma cells.

Complicating the matter further, both hardwoods and softwoods develop “reaction wood” as a response to gravitational or bending forces (Boyd [1977]). In the case of softwoods the reaction is called “compression wood” and forms on the compression side of the stem, closest to the force (inner curve). In contrast, reaction wood in hardwoods is called “tension wood” and forms on the tensional side of the stem, away from the force (outer curve).

In both hardwoods and softwoods the reaction wood is manifested in the fibers or tracheids, respectively. In most hardwoods, tension wood is characterized by the development of an extra innermost layer in the fibers called the gelatinous- or g-layer (Dadswell and Wardrop [1955]). The g-layer is composed mainly of cellulose with a very low MFA, and causes tension wood to exhibit higher than normal cellulose content (Timell [1969]). Tension wood is more difficult to machine and has higher radial-longitudinal shrinkage than normal wood. G-layer development is shown in Figure 4 and the g-layer itself in more detail in Figure 5.

In softwoods compression wood is characterized by a higher than normal lignin content and a higher MFA in the S2 layer of the tracheids (Côté

et al. [1966]). This causes compression wood to exhibit greater longitudinal shrinkage than normal wood.

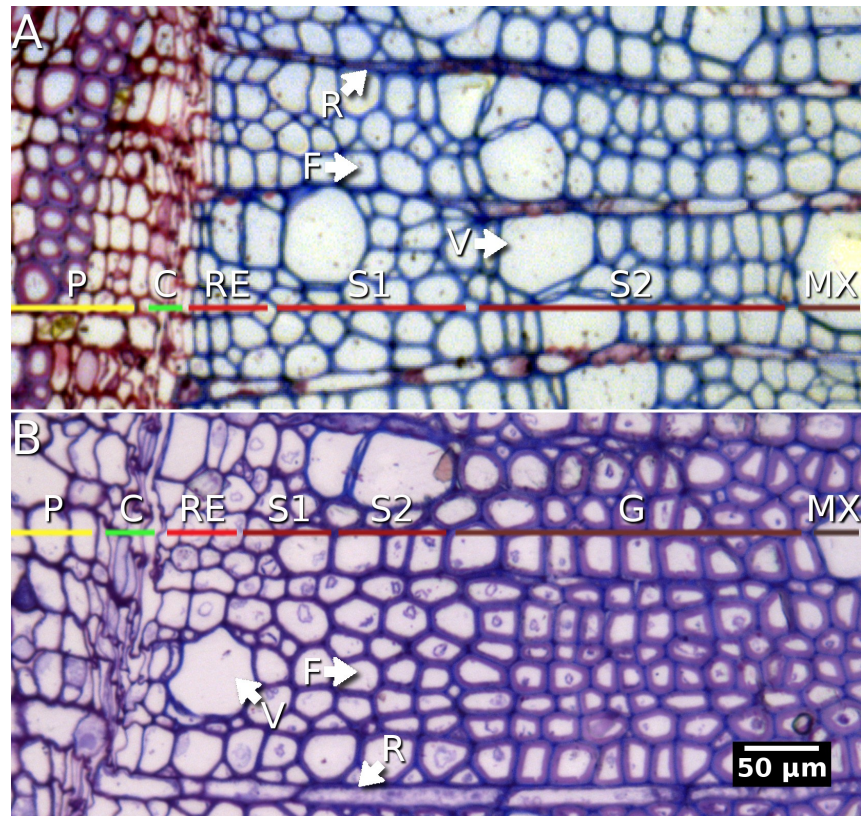


Figure 4: Examples of differentiating normal (A) and reaction wood (B) in aspen. In both images arrows indicate: fibers (F), rays (R) and vessels (V). Indicated along the development line are: phloem (P), cambium (C), radial expansion zone (RE), first secondary layer formation zone (S1), second secondary layer formation zone (S2) and mature xylem (MX). The sections are stained with toluidine blue.

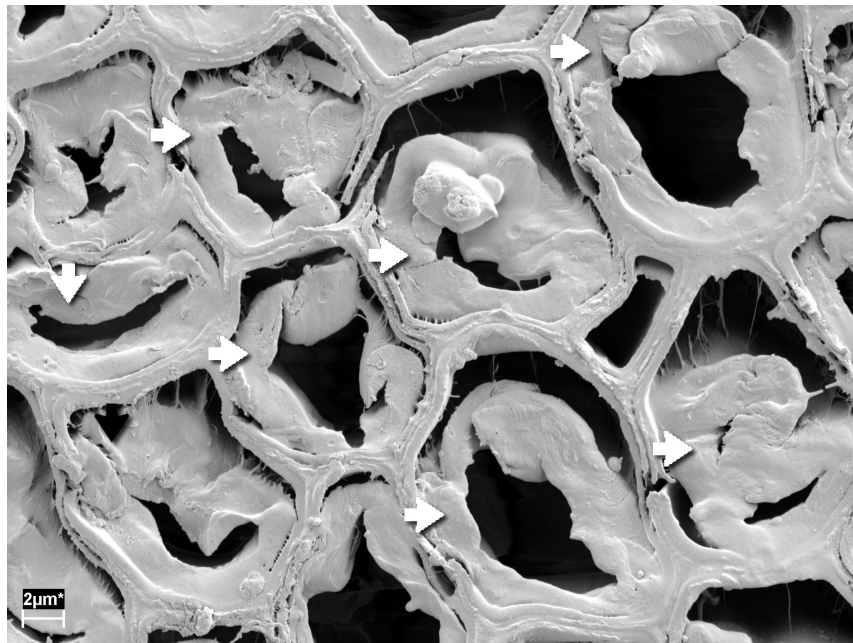


Figure 5: SEM micrograph showing a transverse section of tension wood. The g-layer (arrows) contains little or no lignin which causes much of its gelatinous character. It is also only loosely connected to the outer part of the secondary cell wall.

1.4 Hardwood ultrastructure

There is a boundary which may be defined as the borderline between individual wood cells and wood cell wall. Properties and structure within the cell wall are said to be ultrastructural down to the level of chemical properties and individual molecules. Large ultrastructural differences exist between the different cell types in the xylem of hardwoods such as aspen. Fibers in hardwoods generally exhibit a layered secondary cell wall structure as shown in Figures 6 and 7. An overview of the fiber differentiation (development) process is given in Figures 9A-D.

Individual fibers are joined by the middle lamella (ML) and primary cell walls (PW). Fibers at an early stage of development in the cambium are shown in Figure 9A. Fiber development typically takes place in the radial cell wall prior to the tangential, to maintain the mechanical structure of the cambium. The cellulose microfibrils in the PW do not show any overall organization. The PW contributes very little to the strength of fibers, but contributes to characteristics of fracture propagation throughout the xylem (Gibson and Ashby [1999]).

The middle lamella is composed primarily of lignin and hemicelluloses secreted from the adjacent cells and forms part of the cellular adhesion between cells in the cambium. Where three or more fibers connect, a middle lamella cell corner (MLcc) is formed (Figure 6). The MLcc, depending on size, may show less lignification than the ML and also more electron-lucent areas using transmission electron microscopy (Figure 6).

Fibers normally develop a thick secondary wall inside the primary wall consisting of two separate layers termed S1 and S2, as shown in Figures 6 and 7. Both S1 and S2 exhibit an extremely well organized microfibril structure with very characteristic MFAs. The microfibrils circle the fiber in opposite directions in S1 and S2 layers (Figure 8), with a characteristically low MFA in S2 with reference to the perpendicular axis of the fiber. In some hardwoods an S3 layer may also be present on the inside of the S2 layer. However, as shown in Figure 6 such a layer is not readily apparent in aspen.

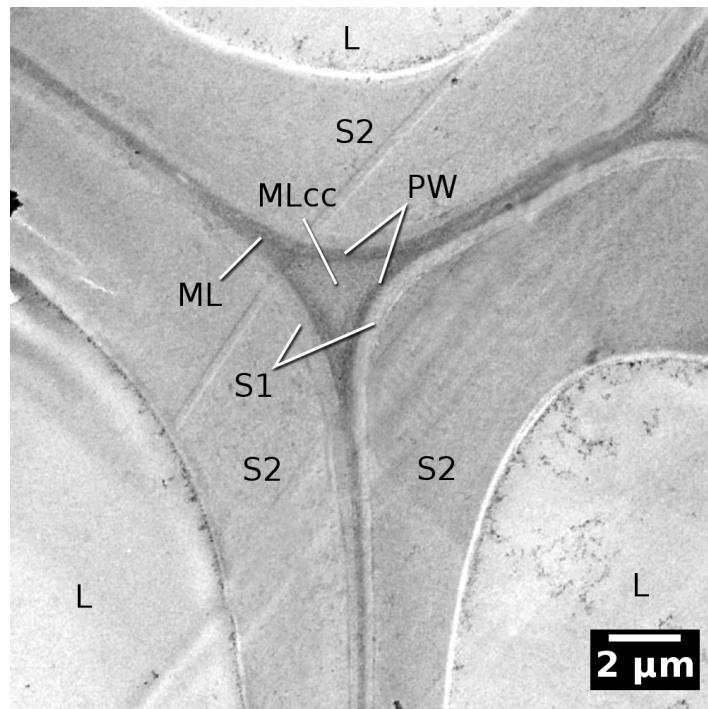


Figure 6: TEM micrograph of a transverse section of the cell corner of 3 aspen fibers. The secondary fiber cell wall is composed of two layers (S1 and S2) that are “glued” together via the compound lamella composed of two primary cell walls (PW) and middle lamella (ML). At the fiber junction, a middle lamella cell corner (MLCC) region is formed, which exhibits special properties. Each fiber shows an empty lumen (L).

The tubular shape of a fully differentiated fiber is shown in Figures 7, 9C and D. The fiber is dominated by the thick secondary S2 cell wall and a large, empty cell lumen when mature. Mechanical properties of the fibers, and in turn the xylem, are largely determined by the properties of the S2 layer. Fracture properties are however influenced to a large degree by the properties of the PW/ML as this represents the weakest point between fibers (Gibson and Ashby [1999]).

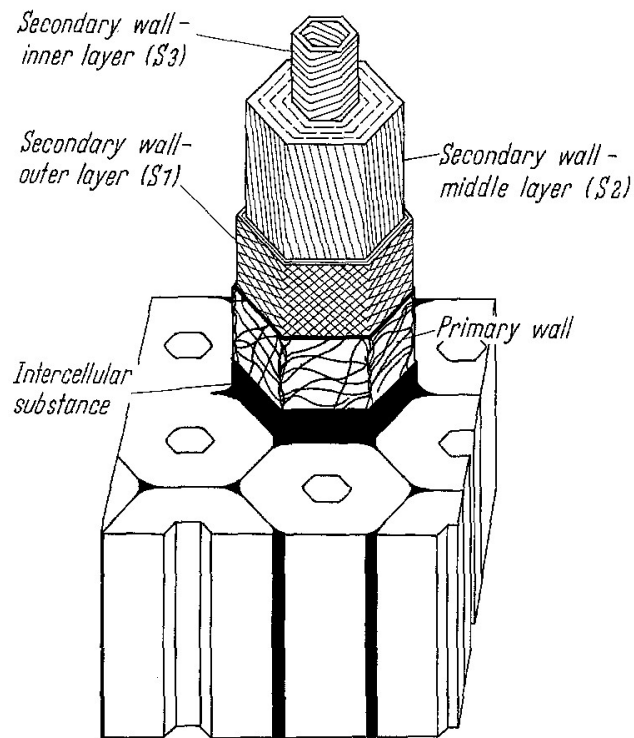


Figure 7: Schematic illustration of the separate layers in the fiber cell wall, adopted from Timell [1967]. Lines within the primary and secondary (S1, S2, S3) cell walls reflect the postulated MFA of the cellulose microfibrils.

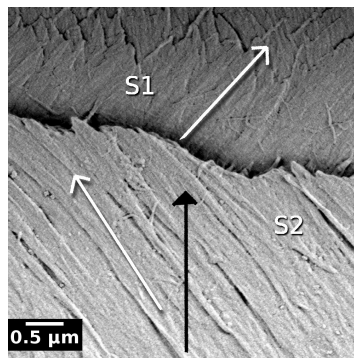


Figure 8: SEM micrograph showing the different MFAs (white arrows) of the secondary cell wall layers of aspen (S1 and S2). Black arrow indicates main fiber axis.

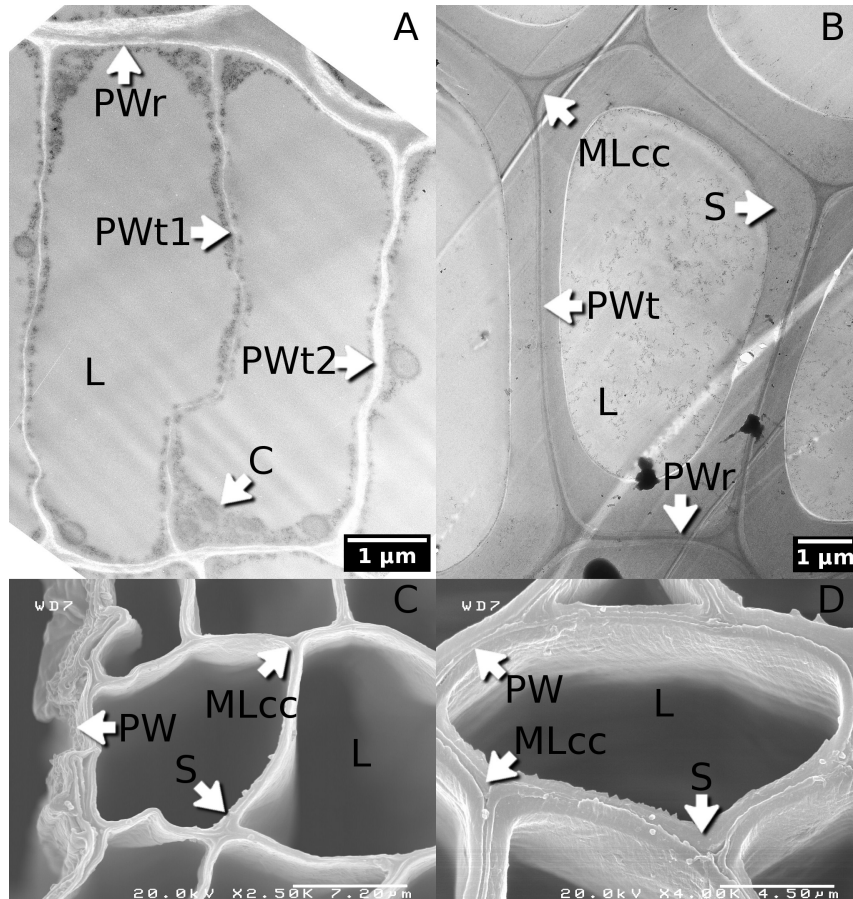


Figure 9: Montage illustrating fiber development. Fibers are continuously formed in joint succession in the cambium as shown in (A). Here, a thick radial cell wall (PWr) is maintained as mechanical necessity, with sequentially forming tangential walls developing thereafter (compare PWt1 and PWt2). After the PW has developed, each of the secondary cell walls (S) develop in turn as the cell wall thickens, as shown in (C) and (D). A fully differentiated fiber (B) consists mainly of a secondary cell wall layer (S) composed of a thick S2 layer and a thinner S1 layer. Abbreviations: cell lumen (L), cytoplasm (C), primary cell wall, radial (PWr) and tangential (PWt), secondary cell walls (S), middle lamella cell corner (MLcc). A,B show TEM- and C,D SEM images.

1.5 Chemical composition

At a molecular level, wood is composed of three major architectural components, namely cellulose, lignin and hemicelluloses. In addition to these components, wood frequently contains “extractives”, composed of low molecular components that can be removed with solvents. Hemicelluloses are a large group of different often highly specialized polysaccharides, mainly consisting of glucose, xylans and mannans. Pectins are similar in composition to hemicelluloses and are sometimes included in the hemicellulose group. In an analogous way to a man-made composite, lignin forms the polymer matrix, cellulose acts as the fiber reinforcement and hemicelluloses the softening agent.

The distribution of these components is different between hardwoods and softwoods and also varies between wood species. In Table 1 the chemical composition for mature *Populus tremuloides* is given.

Cellulose	Lignin	Xylan	Mannan	Pectin, ash, etc.
48	21	24	3	4

Table 1: Chemical composition (%) of *Populus tremuloides* (Timell [1967]).

Cellulose

Cellulose¹ is a linear, polysaccharide composed of β -(1 \rightarrow 4) linked D-glucose units (Figure 10) (Gardner and Blackwell [1974b]). The macromolecular nature of cellulose was first proposed by Staudinger [1920], corroborated by Sponsler and Dore [1926] via x-ray crystallography and later confirmed by Meyer and Misch [1937]. Although simple in chemical composition, it is the linear and regular structure of cellulose that gives it the ability to form tightly packed crystalline complexes held together with hydrogen bonds (Gardner and Blackwell [1974a,b]). The strength of cellulose does not come from its individual chains, but rather from the crystalline complexes. It should be noted that the finer aspects of cellulose superamolecular structure have been further refined since these early publications (O’Sullivan [1997]).

¹from French, *cellule*, biological cell

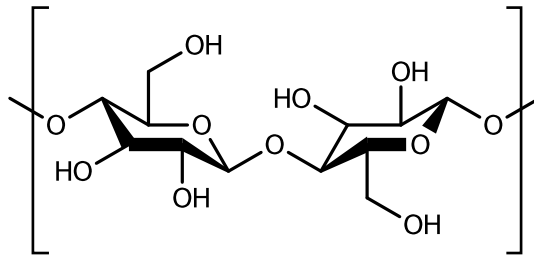


Figure 10: Molecular structure of cellulose (cellobios repeating unit shown), consisting of β -(1 \rightarrow 4) linked D-glucose units (Gardner and Blackwell [1974b]).

Cellulose biosynthesis occurs in the cell plasma membrane by complexes of CesA proteins which form rosette complexes, commonly referred to as the “cellulose rosette” (Mueller and Brown [1980], Brown and Saxena [2005]). From the rosette a number of cellulose microfibrils are spun directly into the cell wall in unison forming a microfibril (Figure 11) (Frey-Wyssling [1948, 1954], Delmer and Amor [1995]). It is proposed that the microfibrils naturally aggregate in to macrofibrils, of varying sizes for different organisms (Donaldson [2007]). During cell wall formation, numerous rosettes are also thought to operate in unison. As the microfibrils are deposited they are coated with hemicelluloses, which is later infused with lignin monomers and polymerized.

At the macromolecular level, the exact ultrastructural arrangement between cellulose, lignin and hemicelluloses in the cell wall is still unknown and it has proven difficult to probe the delicate architecture without modifying it. The packing, size and overall order of these macrofibrils and their relation to the other components in the cell wall is still open to debate and three of the proposed structures are shown in Figure 12.

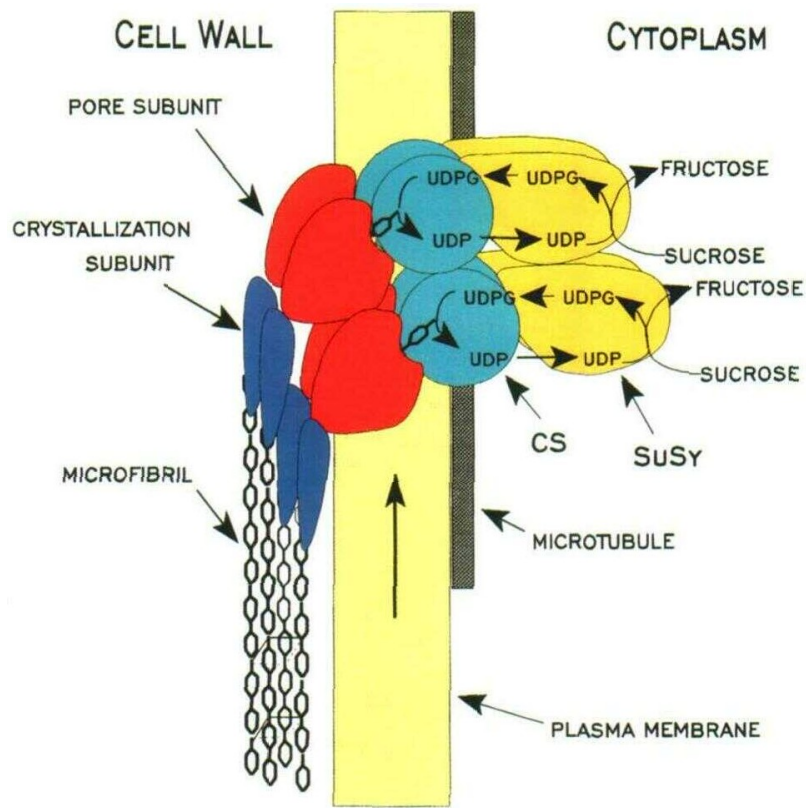


Figure 11: Proposed model of cellulose synthases complex with forming cellulose microfibril (Delmer and Amor [1995]). Abbreviation: catalytic subunit (CS), sucrose synthase (SuSy).

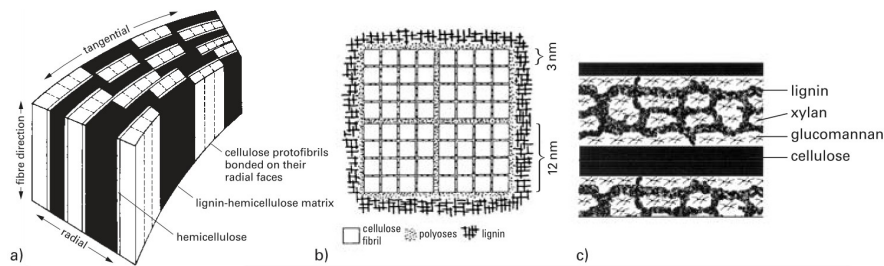


Figure 12: Three proposed models for the ultrastructure of wood with the cellulose microfibrils surrounded by hemicellulose and lignin. (a) Kerr and Goring [1975], (b) Fengel and Wegener [1989] and (c) Salmén and Olsson [1998].

Lignin

Lignin² is a complex “bio-thermoset” phenolic polymer derived from three basic monomers in the plant. It is one of the few natural polymers without a regulated architecture, contributing to its complexity (Boerjan et al. [2003]). The three monomers of lignin are *p*-coumaryl alcohol, coniferyl alcohol and sinapyl alcohol (Figure 13) (Freudenberg [1965]). The monolignols are produced in the cytoplasm through monolignol biosynthetic pathways and transported to the cell wall, possibly in glycosylated form but this has yet to be fully established (Takabe et al. [2001], Boerjan et al. [2003]). The monolignols are in turn incorporated in the matrix as *p*-hydroxyphenyl (H), guaiacyl (G), and syringyl (S) lignin, respectively (Freudenberg [1965], Hwang et al. [1990]). The lignification process initiates in the middle lamella cell corners, extending and connecting through the middle lamella, surrounding the developing cell and following the secondary cell wall inwards (Fujita and Harada [2001]).

Syringyl lignin is more easily degraded and depolymerized than guaiacyl lignin, and the syringyl to guaiacyl ratio (S/G) is therefore an interesting characteristic of wood (Fukushima [2001]). The S/G ratio for example gives a relative measure of how resistant a wood species is against chemical or biological lignin degradation.

While cellulose contributes strength to wood, lignin contributes hydrophobicity and resistance to degradation. Without lignin, wood would be similar to cotton. Specifically, lignin is a recalcitrant component that needs to be removed during industrial cellulose recovery and the lignification pathway was initially the most intensely studied part of wood formation (see Section 1.6 for further details).

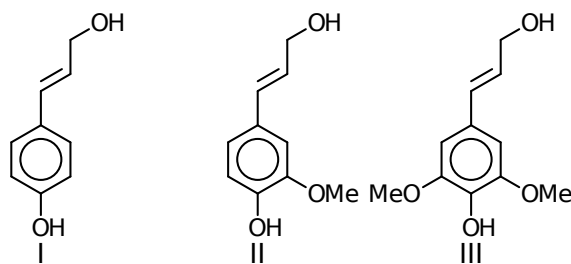


Figure 13: Lignin monomers: *p*-coumaryl alcohol (I), coniferyl alcohol (II) and sinapyl alcohol (III) (Freudenberg [1965]).

²from Latin, *lignum*, wood

Xyloglucan

Xyloglucan (Figure 15) is the most abundant hemicellulose in the primary cell wall of dicotyledons making up 20-25% of its dry weight (Fry [1989]). Xyloglucan has a natural affinity towards cellulose and interacts intimately with the cellulose microfibrils. It has been suggested that amorphous xyloglucan acts as bridging agent between separate cellulose chains and fibrils, allowing the stiff cellulose fibrils to pack more tightly (Fengel and Wegener [1989]). With this close interaction, it is also probable that xyloglucan partly dictates cell wall extensibility and rate of cell expansion (Fry [1989]). As suggested by Mellerowicz et al. [2008], xyloglucan may hypothetically also act as the conductor of tensional force between the g-layer and the surrounding S2 layer in hardwoods.

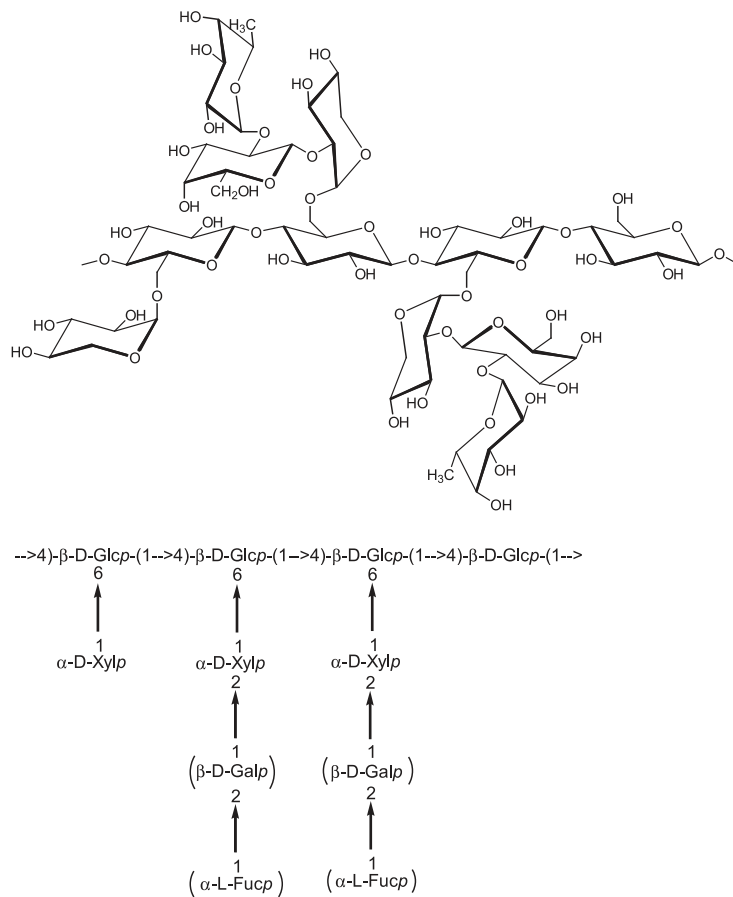


Figure 15: Example of xyloglucan structure (Teleman [2009]).

Pectins

Pectins are a diverse and complex group of polysaccharides making up approximately 4% of the dry weight in aspen (Table 1). Like hemicelluloses, pectins are synthesized in the Golgi apparatus and transported to the cell wall via vesicles. However, unlike hemicelluloses pectins are largely restricted to the primary cell wall, where they help determine cell wall porosity and regulate intercellular adhesion (Willats et al. [2001]).

Pectins can be subdivided into the four major domains homogalacturonan, xylogalacturonan and rhamnogalacturonans I and II (Willats et al. [2001]). The relative abundance of these groups varies, but rhamnogalacturonan I and homogalacturonan are the most common (Schellera et al. [2007]). Rhamnogalacturonan I has a backbone consisting of the disaccharide α -(1 \rightarrow 4)-galacturonic acid- α -(1 \rightarrow 2)-rhamnose, whereas all other pectins contain a linear backbone of α -(1 \rightarrow 4)-linked galacturonic acid (Figure 16). Homogalacturonan exists in multiple esterified forms with mostly unesterified pectin being the dominant in aspen as suggested by Siedlecka et al. [2008]. Arabinogalactan is a subgroup within the rhamnogalacturonan I domain decorated with a galactose-arabinose side chains.

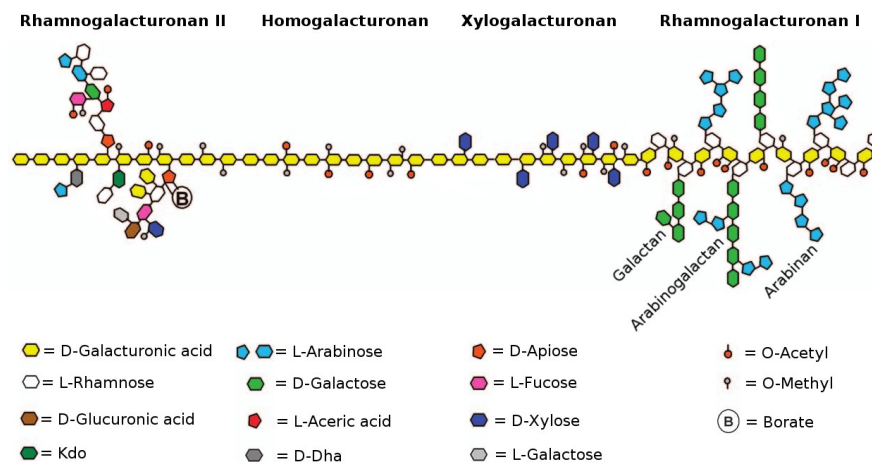


Figure 16: Schematic representation of the pectin domains homogalacturonan, xylogalacturonan, rhamnogalacturonan I and II. Rhamnogalacturonan I and homogalacturonan are the most common pectin domains. Adopted from Schellera et al. [2007].

1.6 Poplar genotypes as model system

Most of the early research on genetic engineering of trees has been conducted using Poplar as a model system because of the species rapid growth, relatively small genome and early genome sequencing, thereby simplifying the production of transgenic plants (Tuskan et al. [2003], Hu et al. [1999], Li et al. [2003], Boerjan et al. [2003]). It has been envisaged that rapid growing Poplar customized through genetic engineering could potentially be a useful resource to meet future increased demands for bioenergy, pulp and paper.

Presently the main application of Poplar genotypes, together with Arabidopsis (“backtrav” in Swedish), is knowledge transfer of genomic effects. Even though this is still a relatively young field, it is envisaged that the knowledge gathered in Arabidopsis and Poplar will be transferable to other wood species such as spruce, acacia and eucalyptus. It could then serve as a reference and complement existing tree breeding programs allowing earlier selection of standard trees with better understanding of their properties.

As lignin is a recalcitrant component in wood that is costly and arduous to remove during cellulose refining it has received the majority of the initial focus of transgenic wood studies (Hu et al. [1999], Li et al. [2003], Chiang [2002], Vanholme et al. [2008], Baucher et al. [2003]). The major industrial potential of the modification/reduction of lignin in trees in both content and composition was thus realized quite early on and much research has since been orientated to understanding the biosynthetic pathways of lignin metabolism in trees with this purpose in mind (Boerjan et al. [2003], Vanholme et al. [2008], Baucher et al. [2003]). One of the major early findings was demonstration in transgenic Poplar that repression of lignin biosynthesis also promotes cellulose accumulation and growth (Hu et al. [1999], Li et al. [2003]).

Despite the intense research on lignin biosynthesis in Poplar species, fewer studies appear however to have concentrated on the morphological affects on wood anatomy, spatial changes in lignin in relation to ultrastructure or physical properties cause by modifications in lignin biosynthesis (Horvath et al. [2010], Leple et al. [2007], Horvath and Peszlen [2010]).

When searching for gene candidates for genomically regulated wood formation responses of interest, there are two options available. From a well characterized pathway a suitable gene can be selected and modified, and hypothesized effects are investigated in genotype plants. Alternatively, if very little prior information is available, screening studies can be made of genome areas of interest. Candidate genes for further study can then be selected based on characterization and evaluation of the produced genotypes

from the screening study.

The candidate genotypes in this thesis were selected based on a screening study initiated by scientists at UPSC and SweTree Technologies AB, and later repeated by Björn Sundbergs group at UPSC. Screening selection was based on significantly modified genotypes based on pyrolysis, klason lignin and fiber master measurements. Initially very little was known regarding the gene function of these genotypes, and still today for most of these genotypes the actual gene function in Poplar is still not clearly defined.

Concurrent with the work in this thesis, these genotypes are also being characterized by UPSC scientists for NMR profiles, wet chemistry, GC-MS pyrolysis and FT-IR composition.

2 Main objectives

The main objective of this thesis was to enhance the current understanding of wood biosynthesis by studying molecular micro-distributions in native and genetically modified aspen (*Populus tremula x tremuloides*). Initial focus was placed on evaluating and refining methods and tools available for labeling (immuno and histochemical) and quantification of wood sample components using fluorescence and electron microscopy, including characterization of the developing fiber cell wall.

Subsequently, focus was placed on applying these tools in a comparative study of down regulated Poplar genotypes. Selection of these previously un-investigated genes and genotypes was made together with UPSC and SweTree Technologies. Finally, focus was placed on a specific study of the micro-distribution of xyloglucan at the ultrastructural level in tension- and normal wood of aspen.

3 Materials and methods

3.1 Genetic transformations

Selection of target genes and genetic transformation was carried out by Umeå Plant Science Centre and SweTree Technologies. Identifiers for the genes and constructs included in this thesis are shown in Table 2. For more information regarding genetic transformation see Paper II page 3.

3.2 Plant material

Wild type and genetically transformed hybrid aspen (*Populus tremula* x *tremuloides*) used for this thesis were clonally propagated in vitro in MS medium (Murashige and Skoog [1962]). After propagation, the plants were transferred to sterilized soil and grown in a greenhouse with an 18-h photoperiod. Natural daylight was supplemented with light from HQI-TS 400W/DH metal halogen lamps (Osram, Munich, Germany). The trees were planted in groups at different times, all groups being accompanied with non-transformed wild type trees. The trees were rotated in the greenhouse to minimize induced systematic errors and the final trees were randomly selected from a large pool of trees.

A few tension wood induced wild type trees together with wild type references were grown under similar conditions in a climate chamber with 16-h photoperiod. To induce tension wood formation, randomly selected plants were inclined at a 30° angle for 2 months before harvest. Again, the trees were rotated in the greenhouse to minimize induced systematic errors.

Samples for SEM labeling were collected from 6 months old trees and cut at 20 cm above soil level from tension wood and non-tension wood stems. From these sections, small cubes (3-mm sides) of fresh wood containing cambium were cut and processed according to the protocol described in Paper IV page 799.

3.3 Immunolabeling for fluorescence and electron microscopy

Immunolabeling was carried out with a range of (primary) antibodies and one CBM shown in Table 3. Depending on the microscopy technique applied, an FITC-conjugated secondary antibody was used for fluorescence microscopy whereas a gold-conjugated antibody was used for electron microscopy. For SEM, gold particles were enhanced with silver to allow detection at SEM resolution (Amersham Biosciences, AuroProbe LM and IntenseSEM).

Construct	PU No.	POPTR ID	Annotation
KR016	PU02990	POPTR_0008s02650.1	ATCSLA09; mannan synthase/transferase
KR100	PU00831	POPTR_0017s05770.1	pfkB-type carbohydrate kinase family protein
KR126	PU01245	POPTR_0014s07670.1	LM domain-containing protein
KR129	PU01524	POPTR_0001s10120.1	Disease resistance-responsive family or dirigent family protein
KR143	PU02081	POPTR_0014s11000.1	SAM-2 (S-ADENOSYLMETHIONINE SYNTHETASE 2)
KR151	PU02254	POPTR_0001s43940.1	Quinone reductase family protein
KR165	PU02482	POPTR_0017s05770.2	pfkB-type carbohydrate kinase family protein
KR175	PU03034	POPTR_0001s09090.1	Remorin family protein
KR213	PU00627	POPTR_0015s09930.1	Pectate lyase family protein
KR015	PU02944	POPTR_0008s00710.1	Glycosyltransferase family 14 or core-2/1-branching enzyme family protein
KR080	PU00489	POPTR_0003s07230.1	UTP-glucose-1-phosphate uridylyltransferase family protein
KR183	PU00145	POPTR_0008s05450.1	Unknown protein

Table 2: Identifiers for genotype constructs used in the thesis. For more information see the Populus database www.populus.db.umu.se



Figure 17: Genotypes KR112, KR139 and KR213 growing together with the wild type reference in the greenhouse at SLU, Umeå, Sweden. The photo was taken just before harvesting at 3 months of age in April 2010 and the plants were approx. 1.5 m tall. Note the characteristic broad juvenile aspen leaves.

The approach was similar for CBM-labeling with the addition of a primary antibody to detect the CBM, before applying a FITC-conjugated or gold-conjugated secondary antibody. Control samples were labeled in parallel with omission of the primary antibody or CBM.

Protein	Epitope recognized	Reference
CCRC-M1 [†]	Xyloglucan	Puhlmann et al. [1994]
CCRC-M8 [†]	Arabinogalactan	Puhlmann et al. [1994]
JIM-5 [†]	Unesterified homogalacturonan ^a	Knox et al. [1990]
JIM-7 [†]	Methyl-esterified homogalacturonan ^a	Knox et al. [1990]
LM-10 [†]	Xylan	McCartney et al. [2005]
FXG-14b [‡]	Fucosylated xyloglucan	Cicortas Gunnarsson et al. [2004]

Table 3: [†]Antibodies and [‡]CBM used for immunolabeling. ^aThis is a simplification regarding the specificity of these two antibodies. For a more complete overview regarding their specificities see Clausen et al. [2003].

3.4 Electron microscopy

Both TEM and SEM were employed to study different ultrastructural properties, and used in combination with immunogold labeling to study carbohydrate spatial micro-distributions during wood differentiation.

SEM observations were made using an Hitachi FE-SEM operated at 20 kV. TEM observations were made using a Philips CM/12 transmission electron microscope (TEM) operated at 80 kV.

3.5 Fluorescence microscopy

Sequential fluorescence microscopy images were collected using a wide-field Leica DMRE fluorescence microscope fitted with a mercury lamp and I3-513808 filter-cube (Leica, excitation 450-490 nm, emission >515 nm) (Leica Microsystems, Wetzlar, Germany). “Dual acquisition” trials with FluoroJ were conducted on a inverted Leica DMRE wide field fluorescence microscope equipped with a structural light unit that allows confocal images (Leica Microsystems, Wetzlar, Germany), equipped with 405, 458, 477, 488, 514, 543 and 633 nm filters (Chroma Technology, Bellows Falls, USA).

Images for coverage quantification were collected using sequential images taken in the green spectrum. Lignin in wood has a strong autofluorescence in the blue spectrum gradually decreasing into red. Unfortunately, the emissions from the mercury lamp have a peak in the red spectrum, which effectively masks autofluorescence and immunofluorescence signals. Therefore, the best “trade off” using a fluorescence microscope fitted with a mercury lamp is to use a FITC fluorophore in the green spectrum.

3.6 Light microscopy

Light microscopy together with histochemistry was used as an aid for morphological characterisation, detection of g-layer and investigation of the spatial microdistribution of cell wall components. The chemical stains utilized are shown in Table 4.

Stain	Reactant	Reference
Toluidine Blue	General stain	Chaffey [2002]
Safranin + Astra Blue	Lignin, cellulose	Chaffey [2002]
Phloroglucinol	Lignin	Chaffey [2002]
Mäule reaction	Syringyl lignin	Chaffey [2002]

Table 4: Chemical stains used in the thesis

3.7 Image analysis

As part of this thesis, an ImageJ (Abramoff et al. [2004]) plugin and protocol called FluoroJ was developed (paper I). The aim of the plugin was to aid quantification of fluorescence images and to minimize supervisor bias. As a basis, FluoroJ uses a slightly altered Difference of Gaussians (DoG) algorithm to isolate the sought (i.e. specific) immunofluorescence from the background autofluorescence signal. Autofluorescence primarily emitted from lignin is almost always present in fluorescence microscopy of woody material. The influence of autofluorescence may be minimized, but very seldom eliminated. FluoroJ instead uses autofluorescence as a reference for calculating signal coverage.

The DoG algorithm is mainly used for image enhancement (sharpening) and edge detection in image analysis and computer vision. The basic principle of DoG is subtraction of a Gaussian blurred image version of a image from a less blurred version. The size ratio between the two kernels, as well as absolute kernel sizes will affect which scale of objects are being sharpened. When used as an approximation of the Laplacian of Gaussian for edge detection, the ratio is typically 1.6 (Marr and Hildreth [1980]). Alternatively, when used for image enhancement the ratio is typically between 4 and 5. FluoroJ uses a ratio of 1.6, and the absolute sizes of the kernels must be tuned to the resolution and sample being observed.

The FluoroJ protocol and plugin work by acquiring two images of the same area of interest. One image containing a complete image of the reference area of interest (“reference”), and one of the same area but with signal or stain added to the area (“signal”). In the case of wood xylem, the reference area is typically the full tissue area. The signal is then isolated from the background by DoG subtraction. The resulting image and a copy of the reference is then thresholded to isolate the fluorescence signals in both. For the sake of statistical comparison, FluoroJ then calculates a coverage fraction. This is simply the amount of isolated signal area divided by the amount of isolated reference area.

Mathematically DoG approximates the “Mexican Hat” wavelet and the DoG convolution kernel is expressed as:

$$DoG \triangleq G_{\sigma_1} - G_{\sigma_2} = \frac{1}{2\pi} \left[\frac{1}{\sigma_1} e^{-(x^2+y^2)/2\sigma_1^2} - \frac{1}{\sigma_2} e^{-(x^2+y^2)/2\sigma_2^2} \right] \quad (1)$$

where:

- x, y = spacial coordinates
- σ_1 = narrow Gaussian kernel or standard deviation
- σ_2 = wide Gaussian kernel or standard deviation

3.8 Statistical analysis

In order to effectively compare the different genotypes, groups and lines to the wild type, it was necessary to conduct both univariate and multivariate statistical analysis. This allows both for a solid overview of genotype effects in combination with detailed information of specific effects. By including the different groups in the model (pooling the variances) it is possible to greatly enhance the estimates of variances and acquire much more reliable results. In the univariate case, the model used is expressed as:

$$y_{ijkm} = \mu + \alpha_i + \gamma_{ij} + \ell_{ijk} + e_{ijkm} \quad (2)$$

where:

- μ = overall mean
- α_i = (fixed) effect of group (A, B or C); $i = 1, 2, 3$
- γ_{ij} = (fixed) effect of genotype j within group i ; $j = 0, \dots, n_i$,
 $n_1 = 9, n_2 = 3, n_3 = 3$
- $\ell_{ijk} \sim N(0, \sigma_\ell^2)$; (random) effect of line within group and genotype
- $e_{ijkm} \sim N(0, \sigma_e^2)$; (random) residual error

The genotype with subscript $j = 0$ was used as the control within the group. If $\sigma_\ell^2 > 0$, then the precision of the comparison of a genotype against its control, in model terms $\gamma_{ij} - \gamma_{i0}$, is influenced by the variation among the lines in addition to the variation among residual errors. The set of comparisons within a group were adjusted for experiment-wise error by Bonferroni adjustments, i.e. a single difference was considered significant if the p -value was at most $0.05/9 = 0.0056$ in group A or $0.05/3 = 0.0167$ in groups B and C.

Analogous, the multivariate model is a generalization of the univariate case over n dimensions, where dimensions correspond to the number of variables. However, because of dimensional complexity, only physical and

fiber properties were included in the morphological multivariate analysis. The equivalent multivariate model is expressed as:

$$\begin{bmatrix} y_{ijkm}^{(1)} \\ \vdots \\ y_{ijkm}^{(n)} \end{bmatrix} = \begin{bmatrix} \mu^{(1)} \\ \vdots \\ \mu^{(n)} \end{bmatrix} + \begin{bmatrix} \gamma_{ij}^{(1)} \\ \vdots \\ \gamma_{ij}^{(n)} \end{bmatrix} + \begin{bmatrix} \ell_{ijk}^{(1)} \\ \vdots \\ \ell_{ijk}^{(n)} \end{bmatrix} + \begin{bmatrix} e_{ijkm}^{(1)} \\ \vdots \\ e_{ijkm}^{(n)} \end{bmatrix} \quad (3)$$

where n is the number of dimensions/variables, $\mu = [\mu^{(1)}, \dots, \mu^{(n)}]'$ is the vector of overall means, $\gamma_{ij} = [\gamma_{ij}^{(1)}, \dots, \gamma_{ij}^{(n)}]'$ is the vector of genotype effects, $j = 0, \dots, m_i$, $m_1 = 9, m_2 = 3$ are the fixed effects (genotypes in group A and B, respectively). The vectors of random effects for line and residual variation $\ell_{ijk} = [\ell_{ijk}^{(1)}, \dots, \ell_{ijk}^{(n)}]'$ and $e_{ijkm} = [e_{ijkm}^{(1)}, \dots, e_{ijkm}^{(n)}]'$ are assumed to follow multivariate normal distributions with mean vectors 0 and covariance matrices:

$$\Sigma_\ell = \begin{bmatrix} \sigma_\ell^2(1) & \sigma_\ell(1,2) & \dots & \sigma_\ell(1,n) \\ \sigma_\ell(2,1) & \sigma_\ell^2(2) & \dots & \sigma_\ell(2,n) \\ \vdots & \vdots & \ddots & \vdots \\ \sigma_\ell(n,1) & \sigma_\ell(n,2) & \dots & \sigma_\ell^2(n) \end{bmatrix}$$

$$\Sigma_e = \begin{bmatrix} \sigma_e^2(1) & \sigma_e(1,2) & \dots & \sigma_e(1,n) \\ \sigma_e(2,1) & \sigma_e^2(2) & \dots & \sigma_e(2,n) \\ \vdots & \vdots & \ddots & \vdots \\ \sigma_e(n,1) & \sigma_e(n,2) & \dots & \sigma_e^2(n) \end{bmatrix}$$

respectively. The vectors ℓ_{ijk} and e_{ijkm} are assumed independent.

The model or parts were used for different comparisons. First, to compare the control genotypes of the groups it was possible to simplify the model as the controls with subscript $j = 0$ contained only one line with $k = 1$ implying the line effects $\ell_{i01} = 0$. Thus, the model for this comparison of controls was $y_{i01m} = \mu + \gamma_{i0} + e_{i01m}$ and the test was performed as a T^2 -test, a generalization of the t -test proposed by Hotelling. Secondly, in the complete model there is a risk that the estimates of the components of Σ_ℓ degenerate in which case estimates of the diagonal elements of Σ_ℓ become zero. This was checked by univariate versions of the model, and in the final multivariate model those components for variance and covariances are set to 0.

The comparisons of genotypes versus their group controls were performed by using the multivariate model as well as its univariate versions for

one variable at a time. The test variable for the multivariate comparisons was an approximate F statistic with 5 d.f. in the numerator and for the univariate comparison, a t statistic was used. If the components of Σ_ℓ are non-zero, then the precision of the comparison of a genotype against its control is influenced by the variation among the lines in addition to the variation among residual errors. The set of comparisons within a group were again adjusted for experiment-wise error by the same Bonferroni adjustments.

4 Results and discussion

Throughout the result section **red** values are statistically significant at level 5%. **Blue** values show a statistical tendency of significance with p-value below 10%. Where appropriate, p-values have been adjusted with Bonferroni correction for multiple comparisons within their groups.

During the initial phase of this work it was soon realized that existing techniques for characterization of micro-distribution would not provide enough detail or be too laborious to effectively compare closely related clones, some with very small modifications related to the control. The high sample variability also forced a statistical evaluation, which necessitates quantifiable results. Furthermore, as the level of down-regulation was unknown, line variations were utilized as an estimate of transformation effectiveness.

To facilitate quantifiable results, we decided to develop the novel image analysis protocol presented. There is a lot of truth to the adage "a picture is worth a thousand words", and much image analysis is concerned with variable reduction. This is particularly true for the protocol presented in this thesis, where the number of variables are first reduced to a single set of coordinates and intensities, then further reduced to only two levels of intensities and finally to just a single quantity. Future work plans to expand the considered variables by taking into account cell location and its associated intensity in the statistical evaluation.

As the function of these genes were and still are mostly unconfirmed or unknown in aspen, emphasis for the micro-distribution characterization was placed on minor cell wall components where it was hypothesized that early signs of modifications would be manifested.

4.1 Quantification of fluorescence images

A major difficulty with microscopical screening is scalability and throughput. For example, for this thesis 117 trees and 12,068 images have been processed and analyzed. Without computational aid in their quantification, evaluating them all would not have been possible. To this end, a novel quantification method called “FluoroJ” was developed as part of this thesis, as outlined in paper I. It’s main goal is to function as a non-biased tool in early screening evaluation together with appropriate statistical modeling.

The FluoroJ protocol allows for both dual and consecutive image acquisition. The results in Paper III were acquired using consecutive image acquisition, an example of which is given in Figure 18. At the moment FluoroJ is best described as a semi-automated quantification technique, particularly in the case of consecutive images.

“Dual image” acquisition (for an example see Paper I, Figure 2, page 8) is a more elegant protocol than consecutive image acquisition and should be the preferable method when available. It minimizes the need for image alignment and simplifies sample handling. Intensity of autofluorescence and image normalization may still prove challenging and have to be taken into consideration. With these considerations in mind consecutive image acquisition was deemed more suitable at the initiation of the project, and later maintained to simplify relational comparability between immunolabels.

Results from testing the protocol against operator supervised (manual) quantification is given in Paper I Figures 4, 5 and 6, page 12. Overall the method compares favorably with manual control, giving correlations (R^2 , explained total variations) between the two methods in the range of $\sim 80\%$ (Paper I, Table 1, page 13). Immunolabeling correlated with anatomical features may introduce added random error, which may decrease correlation and the significance of comparisons. Anatomical variations are not yet accounted for in the method, hence sample size (mean population per sample) was increased for the study in Paper III. This gives more normalized results, better estimates of true coverage and is always recommended when feasible.

Results for quantification of immunolabeling from the antibodies used is given in Table 8, with results from method control (negative) immunolabeling given in Paper III Table 5, Figures 8 and 9, page 12.

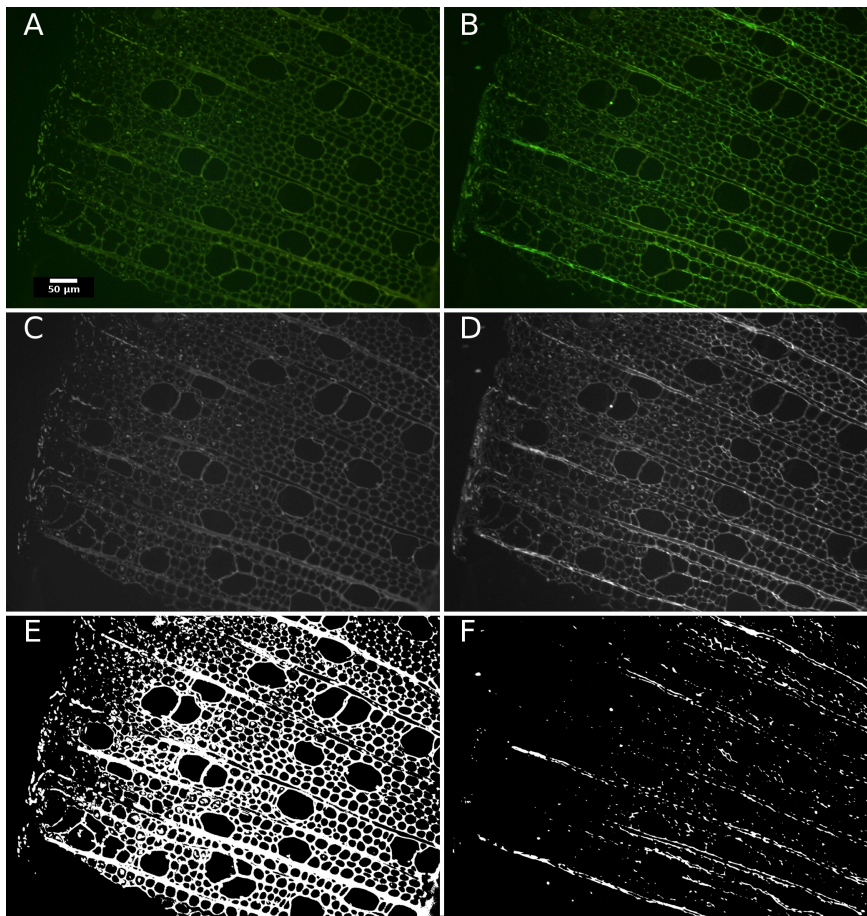


Figure 18: Illustration of the signal isolation by FluoroJ from two consecutive exposures. The two fluorescence images were captured on a wide-field Leica DMRE fluorescence microscope. Both images were taken under the same conditions, the first prior to immunolabeling with CCRC-M1, and the second after labeling. The images have been aligned and normalized. Coverage for this sample is 7.72% (see Paper I, Figures 1 (page 5), 3 (page 10) and Table 1 (page 13) for additional technical detail and Paper III, Table 5, page 10 for coverage evaluation).

4.2 Morphological relationships

The morphological and physical relationships reported in Table 5 can be attributed to known growth patterns of a tree and interdependent developmental fiber traits (Kollmann and Cote [1968]). The statistical evaluation shows a strong significant relationship between tree height and diameter (i.e. quite naturally as the tree grows taller it also grows thicker). Similarly, the evaluation also shows a significant relationship between fiber length and fiber lumen area.

Surprisingly, as no effort was made to select fibers at a specific distance from the pith, the evaluation also show indications of statistical relationships between fiber lumen area – stem diameter and fiber length – tree height. The relationship between increased fiber length and width as a effect of distance from pith has been shown in earlier studies (Kollmann and Cote [1968]), and is actively utilized in the pulp and paper industry were side-cuts of round logs (“bakar” in Swedish) is the main component of “re-inforcement pulp” (“sågverksmassa” in Swedish).

Lastly, related to fiber development, the evaluation shows a significant relationship between radial- and tangential fiber cell wall thickness. This gives an indication of the importance for uniform fiber cell wall development in aspen. Furthermore, the inverted significant relationship between fiber cell wall thickness and fiber lumen area indicates that an increase in fiber cell wall thickness takes place at the cost of fiber lumen area and not overall fiber width.

	Diameter	F. length	F. lumen	F. width	Height	R. thick.	T. thick.
Diameter	-	0.15	0.18	0.09	0.71	0.03	0.04
F. length	-	-	0.23	0.12	0.19	0.04	0.18
F. lumen	-	-	-	0.05	0.05	-0.30	-0.27
F. width	-	-	-	-	0.12	-0.08	-0.13
Height	-	-	-	-	-	0.02	0.01
R. thick.	-	-	-	-	-	-	0.82
T. thick.	-	-	-	-	-	-	-

Table 5: Statistical relationships between morphological measurements based on residual correlations (Paper II). This statistical comparison contains a supplementary dataset of 3 clones not included in Paper II.

4.3 Compositional relationships

Interpretation of coverage relationships after immunolabeling (Table 6), is much more complex than for the morphological properties. The statistical significant relationship shown between CCRC-M1 (xyloglucan) and CCRC-M8 (arabinogalactan) is thought to relate to similar labeling patterns of xyloglucan and arabinogalactan content in the rays (Paper III).

The indication of a statistical relationship between CCRC-M1 and JIM-7 (methyl-esterified homogalacturonan) is thought to be derived from similar labeling patterns of vessels, rays and middle lamella cell corners (MLcc).

Interestingly, the lack of relationship between CCRC-M1 and JIM-5 (unesterified homogalacturonan) is postulated to be caused by JIM-5's stronger signal in the MLcc's than either JIM-7 or CCRC-M1. This would cause JIM-5 to be more influenced by fiber distributions.

Finally, the indication of an inverted statistical relationship between JIM-5 and LM-10 (xylan) may indicate a masking effect between pectins and xylan. Alternatively, as pectins are almost exclusively found in the PW and xylan throughout the cell wall, it may also be an effect of changes in fiber cell wall thickness affecting the relative amount of pectin signal. However, if this is the case this raises questions regarding the lack of a similar relationships for CCRC-M1. The lack of a relationship for arabinogalactan is more easily perceived as the CCRC-M8 signal was almost exclusively found in the ray cell wall in aspen.

	CCRC-M1 xyloglucan	CCRC-M8 arabinogalactan	JIM-5 homogalactur.	JIM-7 Me-homogalactur.	LM-10 xylan
CCRC-M1	-	0.28	0.12	0.25	0.08
CCRC-M8	-	-	0.03	0.12	-0.03
JIM-5	-	-	-	-0.01	-0.25
JIM-7	-	-	-	-	-0.10
LM-10	-	-	-	-	-

Table 6: Statistical relationships between the immunolabeling results based on residual correlations.

4.4 Genotypical influence on morphology

Ultimately, xylem morphology is the sum of its genetic expression. As such, changes in morphology reflects changes in the genome. Unfortunately, any one transgenic modification can have morphological effects at multiple levels.

Of all the morphological and physical traits analyzed, only fiber properties were found to be significantly affected (Table 7, Paper II, Tables 4 and 5, pages 7 and 9). Because of dimensional complexity in multivariate analysis, the statistical evaluation was limited to fiber properties, tree height and diameter. Height and diameter were included despite not showing any individual significances, as they may still contribute important growth aspects to the multivariate evaluation.

The multivariate results show significant differences with much more precision than the individual measurements, mainly because the multivariate analysis are less affected by random errors, particularly when the measurements are connected as in this case.

Construct	Multivar. p-value	F. lumen μm^2	F. length mm	F. width μm	R. thick. μm	T. thick. μm
KR016	0.001	150.1	0.88	38.6	7.28	7.31
KR100	0.001	208.4	0.91	34.0	6.16	5.78
KR126	0.001	148.7	0.87	31.2	8.67	9.01
KR129	0.006	201.6	0.91	34.9	5.90	5.48
KR143	0.318	178.0	0.91	35.4	7.77	7.40
KR151	0.147	171.5	0.90	34.9	8.84	8.53
KR165	0.003	220.6	0.90	35.9	6.29	5.42
KR175	0.358	153.9	0.94	33.3	9.43	8.57
KR213	0.006	126.9	0.92	32.6	9.99	10.02
KR015	0.001	145.0	0.91	38.7	7.09	7.01
KR080	0.001	167.8	0.88	36.3	7.27	6.83
KR183	0.212	148.1	0.88	33.9	10.16	10.00
Literature	-	~191	0.96	-	7.10	7.10

Table 7: Comparison of genotype morphology versus group controls. Means for each fiber measurement and p-values of the multivariate tests. Only selected measurements are shown. For additional information see paper II. Literature values are taken from Lehto [1995].

4.5 Genotypical influence on composition

Multivariate analysis was particularly important for coverage results for two main reasons. Firstly, results from a novel quantification technique requires verification against as large a body of evidence as possible. Secondly, as with any novel technique, there are still minor variational fluctuations in the quantification which the multivariate analysis alleviates.

Of particular note are the results for constructs KR100 and KR126 (Table 8). They exhibit no individual significance, but are sufficiently and consistently different to achieve an overall significant difference. These results would have been overlooked without a multivariate evaluation.

Overall, individual significant differences were only recorded for antibodies LM-10 and JIM-5. The lack of significance in the remaining immunostains is due to random variations. Any random (or systematic) variation not accounted for in the statistical model will end up in the residual, compounded by the number of samples analyzed. An obvious random effect not accounted for is changes in morphology, but work is progressing for an initial solution to this problem (see future work).

Construct	Multivar. p-value	CCRC-M1 Xyloglucan	CCRC-M8 Arabinogal.	LM-10 Xylan	JIM-5 Homogalact.
KR016	0.022	0.035	0.109	0.235	0.084
KR100	0.003	0.070	0.106	0.090	0.079
KR126	0.004	0.077	0.107	0.156	0.079
KR129	0.026	0.067	0.134	0.170	0.075
KR143	0.003	0.070	0.129	0.060	0.067
KR151	0.001	0.077	0.121	0.037	0.068
KR165	1E-4	0.049	0.140	0.012	0.059
KR175	0.266	0.082	0.110	0.361	0.078
KR213	0.682	0.057	0.118	0.566	0.102
KR015	0.026	0.087	0.126	0.336	0.044
KR080	0.091	0.059	0.098	0.248	0.047
KR183	0.012	0.041	0.107	0.738	0.159

Table 8: Comparison of genotype coverage versus group controls. Means for each fiber measurement and p-values of the multivariate tests. Only selected measurements are shown. For additional information see paper III.

4.6 Summary of multivariate evaluation

The summarized results of the multivariate evaluations of the 12 genotypes studied in the thesis are shown in Table 9. These results indicate initial trends with genotypes showing differences in either morphology, composition, both or neither.

It is necessary to screen these genotypes using detailed chemotyping and a much larger bank of immunolabeling antibodies (i.e. that target a broader range of epitopes) to say anything definitive regarding chemical and micro-distributional changes in the genotypes.

It is however unlikely that any significant genetic modification only affects an isolated property. The initial supposition is that the genes for the unaffected genotypes do not significantly impact fiber development. They may still display modifications but the present suggestion is that they are minor. The underlying reasons may be numerous, one of which may be close genetic homologs to the down-regulated genes.

The preliminary supposition for genotypes only displaying significant morphological effects is that the targeted genes do not impact chemical or micro-structural composition of the studied epitopes. This could for example be caused by a regression or block at a vital architectural or combinatorial development pathway (rather than a chemical).

On the other hand, for genotypes which only show significant coverage modifications there is an indication that structural pathways are functional but there may be regressions or modifications to a supply pathway. Alternatively, there may also be changes in structural directing components causing modifications in biomatrix composition or masking. More extensive screening would however be necessary in order to conclude if anything has been truly modified.

For the genotypes which showed significant modifications in both morphology and coverage (Table 9), there is a distinct possibility of significant modification in a structure or supply pathway, which causes large scale ultrastructural modifications. How such modifications are manifested in cell wall ultrastructure requires however further study.

Unaffected	Morphology	Coverage	Both
KR213	KR080	KR183	KR165
KR175	KR016	KR151	KR126
KR129	KR015	KR143	KR100

Table 9: Summary table of morphological and coverage effects based on multivariate statistical significance.

4.7 Xyloglucan deposition during aspen wood formation

Xyloglucan forms an essential part of the primary cell wall of most dicotyledon cells (Fry [1989]), with high concentrations in the vessels, rays (parenchyma cells), and primary cell wall of fibers in the xylem of hardwoods. The presence of xyloglucan in the PW and ML of fibers has previously been shown using immunogold labeling (Baba et al. [1994], Bourquin et al. [2002], Nishikubo et al. [2007], Bowling and Vaughn [2008]), with a decreasing concentration in the secondary cell wall. Recently it has also been suggested that xyloglucan may be present in the g-layer, mediating g-layer S2 interactions (Mellerowicz et al. [2008]).

By combining immunolabeling results from two independent xyloglucan probes, antibody CCRC-M1 and CBM FXG-14b, it was possible to show xyloglucan labeling in the PW/ML (Paper IV, Figure 2, page 802) and in the developing g-layer (Figure 19). The PW/ML labeling patterns substantiate earlier micro-distributional reports, and is further strengthened by the high level of agreement between the two probes. Previously not reported were the observations of the presence of xyloglucan in the developing g-layer (Figure 19 black arrows), obtained by the novel application of a CBM for immunolabeling on a ultrastructural level.

Intensities were however still low, and to obtain higher resolution images without interference from the embedding resin, SEM microscopy was combined with silver enhanced immunogold labeling. Because of the lack of resin and minimal processing, SEM images show much higher intensities compared to TEM as shown in Figure 20. A declining trend could be observed with decreasing intensity in labeling from the PW/ML to the g-layer or S2 (Figures 20A, B vs 20C, D and E, F). A break in the trend was observed with an increase in labeling in the boundary layer between the S2 and g-layer (Figure 20F), which supports the hypothesis of Mellerowicz et al. [2008].

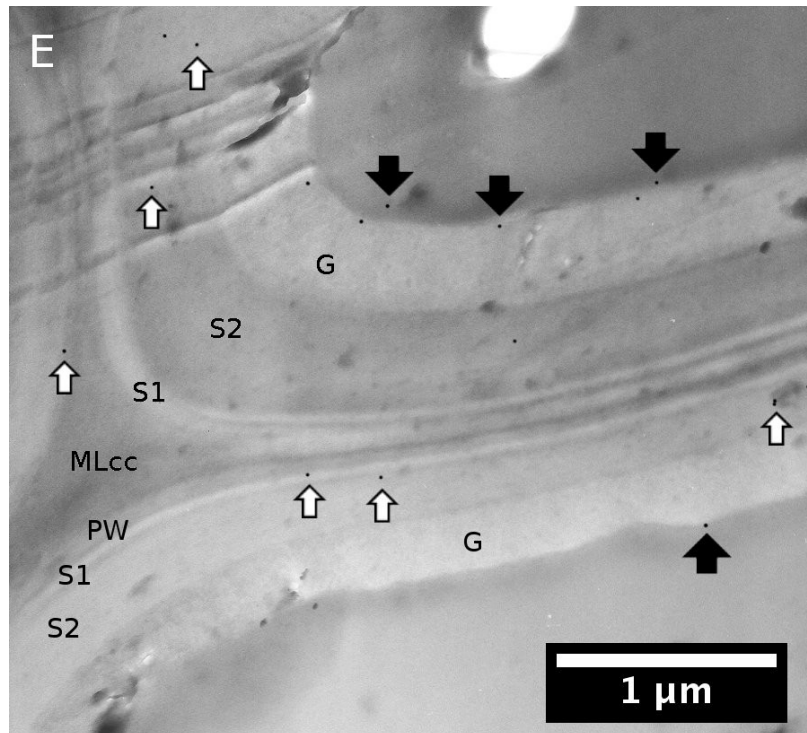


Figure 19: TEM micrograph illustrating xyloglucan presence during g-layer formation as detected with FXG-14b CBM immunolabeling. The immunogold particles are mainly present in the primary cell wall (PW), but were also occasionally be found in the S1 and S2 layers (white arrows). They are also present along the developing g-layer front (black arrows) (Paper IV).

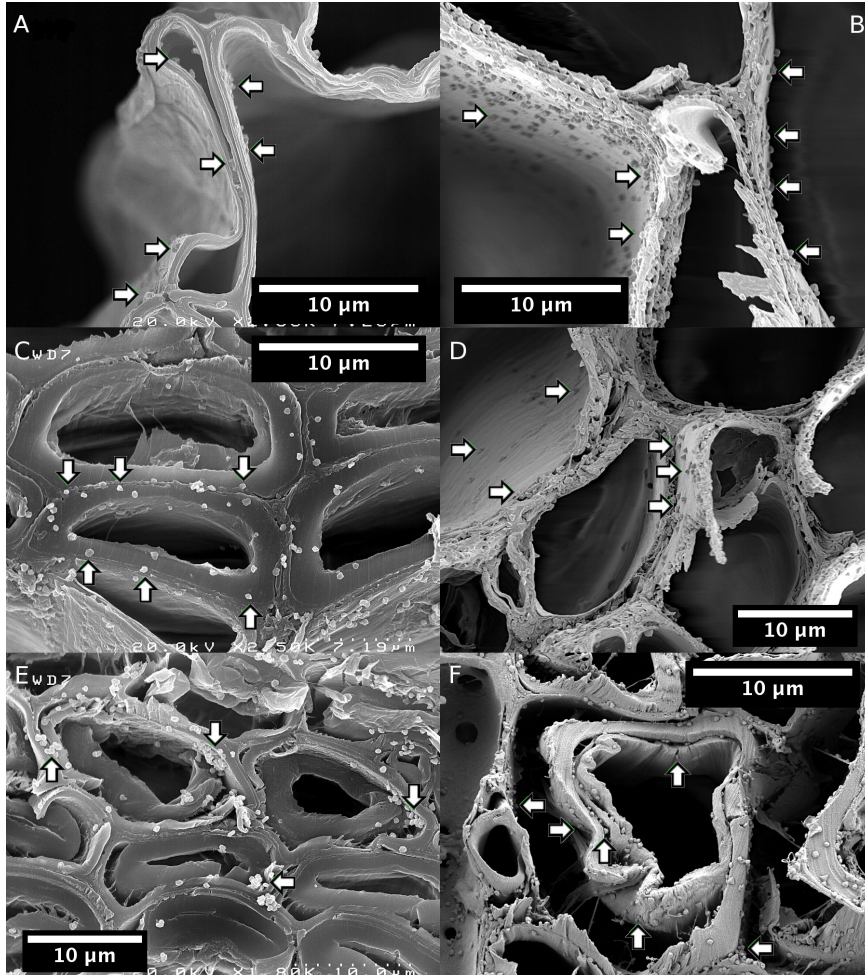


Figure 20: SEM micrographs illustrating xyloglucan presence during wood formation as detected with silver enhanced immunogold labeling using CBM FXG-14b (left column) and antibody CCRC-M1 (right column). Arrows in the images indicate silver particles. Overall there is a very high degree of agreement between the two labels. Strong labeling was recorded throughout the wall at this early stage of development (A and B). Less labeling was detected on the developing S2 layer (C and D). The developing g-layer showed the least amount of labeling, with the exception of the interface between the S2 and g-layer where labeling was often abundant (E and F). See Paper IV for more details.

5 Conclusions

A protocol and ImageJ plugin combination has been developed and successfully applied to semi-automated acquisition of quantitative data from immunofluorescence labeling of wood tissue. In combination with morphological characterization, it can be a valuable addition to semi-high throughput screening of wood tissue. The protocol has been shown to perform favorably compared with operator supervised analysis, and has potential to be further extended for fully automated quantification of wood micro-distribution immunolabeling. The method is not specific to the analysis of genetically modified samples and can readily be applied to non-transgenic wood tissue.

By applying multivariate statistics to morphological and coverage measurements, clearer trends in relationships and properties have been acquired. Specifically, multivariate analysis has been shown to illustrate genotypes with significantly different coverage trends even when no single measurement is significant on its own. Overall, the multivariate analysis confirms expected correlations between individual morphological measurements, and highlights novel coverage relationships.

Detailed morphological characterization (i.e. distribution of cell types, cell wall thickness, etc.) has been shown to be a valuable component in genotypical characterization. Specifically, the impact of anatomical differences should not be underestimated when unraveling global chemical composition. In this thesis, significant changes were however only recorded for fibers and not for vessels.

Using two complementary antibody and CBM probes, evidence for the presence of xyloglucan in the g-layer of tension wood in aspen was obtained. The main concentration of xyloglucan was found in the primary cell wall, with a declining concentration of xyloglucan through the developing secondary wall layers. One exception to the declining trend of xyloglucan was a higher concentration at the interface between the S2 and the g-layer, supporting the hypothesis that xyloglucan acts as an anchor for the g-layer to the inner S2 layer and rest of the secondary cell wall.

6 Future work

Future refinements to the image analysis protocol involves extending the range of immunoprobes and stains and providing more descriptive statistics. By utilizing consecutive image acquisition in light microscopy, preliminary tests have shown that it is possible to extend the FluoroJ protocol to conventional histochemical stains. This would greatly enhance the range of quantifiable labeling techniques and serve as a more general aid in comparisons of microscope images.

Furthermore, refining the signal isolation procedure with cell segmentation and recognition techniques would generate more descriptive statistics on a cell type basis. This would more accurately account for anatomical variations and provide descriptive statistics of modifications both within and between cell types. Segmentation and object recognition is however inherently subject dependent and will require development and optimization for each subject area of interest.

Promising aspen genotypes with improved properties for industrial applications should undergo more in-depth chemical and ultrastructural investigation as well as field trials to evaluate the robustness and potential of the induced genetic modifications. Whether or not field trials and subsequent planting of transgenic trees on a commercial scale is a scientific and political possibility in Sweden is however an open question.

More practically, cross evaluation of the findings in this study with similar genetic, chemical and ultrastructural evaluations of aspen should provide a clearer view of the individual components role in aspen wood formation. This knowledge could then be extended to other wood species of industrial interest and complement existing breeding programs with earlier indications of final properties.

A lot of additional results (e.g. with UV-microscopy, histochemistry, TEM, multivariate analysis) were also obtained on well characterized genotypes that unfortunately are not included in this thesis. Hopefully, this work will also be published in the near future.

References

- M.D. Abramoff, P.J. Magelhaes, and S.J. Ram. Image processing with ImageJ. *Biophotonics International*, 11(7):36–42, 2004.
- K. Baba, Y. Sone, H. Kaku, A. Misaki, N. Shibuya, and T. Itoh. Localization of hemicelluloses in the cell walls of some woody plants using immunogold electron microscopy. *Holzforschung*, 48(4):297–300, 1994.
- R.K. Bamber. Heartwood, its function and formation. *Wood Science and Technology*, 10:1–8, 1976.
- M. Baucher, C. Halpin, M. Petit-Conil, and W. Boerjan. Lignin: genetic engineering and impact on pulping. *Critical Reviews in Biochemistry and Molecular Biotechnology*, 38:305–350, 2003. doi: 10.1080/10409230390242443.
- W. Boerjan, J. Ralph, and M. Baucher. Lignin biosynthesis. *Annual Review of Plant Biology*, 54(1):519–546, 2003.
- V. Bourquin, N. Nishikubo, H. Abe, H. Brumer, S. Denman, M. Eklund, M. Christiernin, T. T. Teeri, B. Sundberg, and J. E. Mellerowicz. Xyloglucan endotransglycosylases have a function during the formation of secondary cell walls of vascular tissues. *The Plant Cell*, 14:3073–3088, 2002.
- A.J. Bowling and K.C. Vaughn. Immunocytochemical characterization of tension wood - gelatinous fibers contain more than just cellulose. *American Journal of Botany*, 95(6):655–663, 2008.
- J.D. Boyd. Basic causes of differentiation of tension wood and compression wood. *Australian Forest Research*, 7:121–143, 1977.
- R.M. Jr Brown and I.M. Saxena. Cellulose biosynthesis: current views and evolving concepts. *Annals of Botany*, 96:9–21, 2005.
- N.J. Chaffey. *Wood formation in Trees*. Taylor & Francis Inc., 2002.
- V.L. Chiang. From rags to riches. *Nature Biotechnology*, 20:557–558, 2002.
- L. Cicortas Gunnarsson, E. Nordberg Karlsson, A. S. Albrekt, M. Andersson, O. Holst, and M. Ohlin. A carbohydrate binding module as a diversity-carrying scaffold. *Protein Eng Des Sel*, 17(3):213–221, 2004.

- M.H. Clausen, W.G.T. Willats, and J.P. Knox. Synthetic methyl hexagalacturonate hapten inhibitors of anti-homogalacturonan monoclonal antibodies LM7, JIM5 and JIM7. *Carbohydrate Research*, 338:1797–1800, 2003. doi: 10.1016/S0008-6215(03)00272-6.
- W.A. Côté, T.E. Timell, and R.A. Zabel. Studies on compression wood - Part I: Distribution of lignin in compression wood of red spruce (*Picea rubens* Sarg.). *European journal of wood and wood products*, 24(10):432–438, 1966.
- H.E. Dadswell and A.B. Wardrop. The structure and properties of tension wood. *Holzforschung*, 9(4):97–104, 1955.
- D.P. Delmer and Y. Amor. Cellulose biosynthesis. *The Plant Cell*, 7:987–1000, 1995.
- L. Donaldson. Cellulose microfibril aggregates and their size variation with cell wall type. *Wood Science and Technology*, 41(5):443–460, 2007.
- D. Fengel and G. Wegener. *Wood: chemistry, ultrastructure, reactions*. Walter De Gruyter, Berlin, 1989.
- K. Freudenberg. Lignin: its constitution and formation from p-hydroxycinnamyl alcohols. *Science*, 148(3670):595–600, 1965.
- A. Frey-Wyssling. The growth in surface of the plant cell wall. In *Growth Symposium*, volume 12, pages 151–169, 1948.
- A. Frey-Wyssling. The fine structure of cellulose microfibrils. *Science*, 119(3081):80–82, 1954.
- S.C. Fry. The structure and functions of xyloglucan. *Journal of Experimental Botany*, 40(210):1–11, 1989.
- M. Fujita and H. Harada. *Wood and cellulosic chemistry*. Marcel Dekker, Inc., New York, 2nd edition, 2001.
- K. Fukushima. Regulation of syringyl to guaiacyl ratio in lignin biosynthesis. *Journal of Plant Research*, 114(4):499–508, 2001.
- K.H. Gardner and J. Blackwell. The hydrogen bonding in native cellulose. *Biochimica et Biophysica Acta*, 343(1):232–237, 1974a.
- K.H. Gardner and J. Blackwell. The structure of native cellulose. *Biopolymers*, 13(10):1975–2001, 1974b.

- L.J. Gibson and M.F. Ashby. *Cellular solids*. Cambridge Solid State Science Series. Cambridge University Press, 2 edition, 1999.
- R.B. Hoadley. *Understanding wood*. Taunton Press, revised edition edition, 2000.
- B. Horvath, I. Peszlen, P. Peralta, B. Kasal, and L. Li. Effect of lignin genetic modification on wood anatomy of aspen trees. *IAWA Journal*, 31(1):29–38, 2010.
- L. Horvath and I. Peszlen. Mechanical properties of genetically engineered young aspen with modified lignin content and/or structure. *Wood and Fiber Science*, 42(3):310–317, 2010.
- W. Hu, S.A. Harding, J. Lung, L. Popko, J. Ralph, D.D. Stokke, C. Tsai, and V.L. Chiang. Repression of lignin biosynthesis promotes cellulose accumulation and growth in transgenic trees. *Nature Biotechnology*, 17: 808–812, 1999.
- R.H. Hwang, J.F. Kennedy, and E.H.M. Melo. A mechanism for lignification in plants. *Carbohydrate Polymers*, 14(1):77–88, 1990.
- H. Juslin and E. Hansen. *Strategic marketing in the global forest industries*. Authors Academic Press, Corvallis, OR, USA, 2003.
- A.J. Kerr and D.A.I. Goring. The ultrastructural arrangement of the wood cell wall. *Cellul. Chem. Technol.*, 9(6):563–573, 1975.
- J.P. Knox, P.J. Linstead, J. King, C. Cooper, and K. Roberts. Pectin esterification is spatially regulated both within cell walls and between developing tissues of root apices. *Planta*, 181:512–521, 1990.
- F.F.P. Kollmann and W.A. Jr. Cote. *Principles of wood science and technology*, volume 1. Springer Verlag, 1968.
- J. Lehto. Various poplar species as raw material for paper grade mechanical pulps. In *1995 International Mechanical Pulp Conference (Ottawa) Proceedings*, page 9, Montreal, 1995.
- J.-C. Leple, R. Dauwe, K. Morreel, V. Storme, C. Lapierre, B. Pollet, A. Naumann, K.-Y. Kang, H. Kim, K. Ruel, A. Lefebvre, J.-P. Joseleau, J. Grima-Pettenati, R. de Rycke, S. Andersson-Gunneras, I. Fehrle, M. Petit-Conil, J. Kopka, A. Polle, E. Messens, A. Erban, B. Sundberg, S.D. Mansfield, J. Ralph, G. Pilate, and W. Boerjan. Downregulation of

- cinnamoyl-coenzyme A reductase in poplar: multiple-level phenotyping reveals effects on cell wall polymer metabolism and structure. *The Plant Cell*, 19:3669–3691, 2007.
- L. Li, Y. Zhou, X. Cheng, J. Sun, J.M. Marita, J. Ralph, and V.L. Chiang. Combinatorial modification of multiple lignin traits in trees through multigene cotransformation. *PNAS*, 100(8):4939–4944, 2003.
- D. Marr and E. Hildreth. Theory of edge detection. *Proceedings of the Royal Society of London Series B*, 207:187–217, 1980. doi: 10.1098/rspb.1980.0020.
- L. McCartney, S.E. Marcus, and J.P. Knox. Monoclonal antibodies to plant cell wall xylans and arabinoxylans. *J. Histochem. Cytochem.*, 53(4):543–6, 2005. doi: 10.1369/jhc.4B6578.2005.
- J. E. Mellerowicz, P. Immerzeel, and T. Hayashi. Xyloglucan: the molecular muscle of trees. *Annals of Botany*, 102:659–665, 2008.
- K.H. Meyer and L. Misch. Positions des atomes dans le nouveau modèle spatial de la cellulose. *Helvetica Chimica Acta*, 20:232–245, 1937.
- S.C. Mueller and R.M. Jr Brown. Evidence for an intramembrane component associated with a cellulose microfibril-synthesizing complex in higher plants. *Journal of Cell Biology*, 84(2):315–326, 1980.
- T. Murashige and F. Skoog. A revised medium for rapid growth and bioassays with tobacco tissue cultures. *Physiologia Plantarum*, 15(3):473–497, 1962.
- N. Nishikubo, T. Awano, A. Banasiak, V. Bourquin, F. Ibatullin, R. Funada, H. Brumer, T. T. Teeri, T. Hayashi, B. Sundberg, and J. E. Mellerowicz. Xyloglucan endo-transglycosylase (XET) functions in gelatinous layers of tension wood fibers in poplar - a glimpse into the mechanism of the balancing act of trees. *Plant Cell Physiol*, 48(6):843–855, 2007.
- A. O’Sullivan. Cellulose: the structure slowly unravels. *Cellulose*, 4:173–207, 1997.
- G. Pilate, E. Guiney, K. Holt, M. Petit-Conil, C. Lapierre, J.-C. Leplé, B. Pollet, I. Mila, E.A. Webster, H.G. Marstorp, D.W. Hopkins, L. Jouanin, W. Boerjan, W. Schuch, D. Cornu, and C. Halpin. Field and pulping performances of transgenic trees with altered lignification. *Nature Biotechnology*, 20:607–612, 2002.

- J. Puhlmann, E. Bucheli, M.J. Swain, N. Dunning, P. Albersheim, A.G. Darvill, and Hahn. M.G. Generation of monoclonal antibodies against plant cell wall polysaccharides. i. characterization of a monoclonal antibody to a terminal alpha-(1,2)-linked fucosyl-containing epitope. *Plant Physiology*, 104:699–710, 1994.
- L. Salmén and A.-M. Olsson. Interaction between hemicelluloses, lignin and cellulose: structure-property relationships. *J. Pulp Pap. Sci.*, 24(3):99–103, 1998.
- H.V. Schellera, J.K. Jensena, S.O. Sørensen, J. Harholta, and N. Geshib. Biosynthesis of pectin. *Physiologia Plantarum*, 129:283–295, 2007.
- A. Siedlecka, S. Wiklund, M.A. Peronne, F. Micheli, J. Lesniewska, I. Sethson, U. Edlund, L. Richard, B. Sundberg, and E.J. Mellerowicz. Pectin methyl esterase inhibits intrusive and symplastic cell growth in developing wood cells of *Populus*. *Plant Physiology*, 146:554–565, 2008.
- O.L. Sponsler and W.H. Dore. The structure of ramie cellulose as derived from x-ray data. In *Fourth Colloid Symposium Monograph*, volume 41, pages 174–202, 1926.
- H. Staudinger. Über polymerisation. *Berichte der deutschen chemischen Gesellschaft*, 53(6):1073–1085, 1920.
- K. Takabe, M. Takeuchi, T. Sato, M. Ito, and M. Fujita. Immunolocalization of enzymes involved in lignification. *Progress in biotechnology*, 18: 177–186, 2001.
- A.M. Taylor, B.L. Gartner, and J.J. Morrell. Heartwood formation and natural durability - a review. *Wood and fiber science*, 34(4):587–611, 2002.
- A. Teleman. *Wood chemistry and biotechnology*. De Gruyter, 2009.
- T.E. Timell. Recent progress in the chemistry of wood hemicelluloses. *Wood Science and Technology*, 1:45–70, 1967.
- T.E. Timell. The chemical composition of tension wood. *Svensk Papperstidning*, 72(6):173–181, 1969.
- G.A. Tuskan, S.P. DiFazio, and T. Teichmann. Poplar genomics is getting popular - the impact of the poplar genome project on tree research. *Plant Biology*, 5:1–3, 2003.

R. Vanholme, K. Morreel, J. Ralph, and W. Boerjan. Lignin engineering. *Curr. Opin. Plant Biol.*, 11(3):1-8, 2008. doi: 10.1016/j.pbi.2008.03.005.

W.G.T. Willats, L. McCartney, W. Mackie, and J.P. Knox. Pectin: cell biology and prospects for functional analysis. *Plant Molecular Biology*, 47: 9-27, 2001.

Acknowledgements

First and foremost, I owe a great debt of gratitude to my mentor Geoffrey Daniel. Not only has he given me a wonderful introduction to the world of microscopy and wood science, he has shown that the journey is as important as the goal. With a understanding and thoughtfulness that I believed was almost lost to the modern world, he has made even the most difficult tasks surmountable. To have had Geoff as a mentor is nothing short of a privilege.

I also owe a big *thank you* too my co-supervisors Jonas Hafrén and Lada Filonova, without whose encouragement and help this thesis would not have been nearly what it is. In fact, this gratitude must be extended to all the people in the group and in the department, who have all help make these four years some of the most memorable I have had.

For me personally, a great highlight of this thesis was my visit to Keiji Takabe's lab in Kyoto University, Japan, and I want to thank him, Arata, Tatsuya, Kim and the wonderful students in the group for making it both a productive and enchanting visit.

I would also like to thank Björn Sundberg, the plant researchers connected to FuncFiber, and SweTree Technologies without whom this project would simply never have been possible.

And finally, I need to thank my wonderful wife Sanna, my caring family and supportive friends for all the encouragement and understanding under these intense but enormously rewarding years.

FuncFiber Center of Excellence

This work was carried out as part of the FORMAS sponsored FuncFiber center of excellence. FuncFiber consisted of 20 project all focused on further developing our understanding of wood formation from gene expression to ultrastructure. For more information please see the centers homepage at www.funcfiber.se.



Used with kind permission, PhD Comic